DESIGN AND ANALYSIS OF AN AUTOMOTIVE BRAKE DISC ON THE BASIS OF TEMPERATURE DISTRIBUTION

A DISSERTATION

SUBMITTED IN PARTIAL FULFILLMENT OF THE REQUIREMENTS

FOR THE AWARD OF THE DEGREE

OF

MASTER OF TECHNOLOGY
IN
PRODUCTION ENGINEERING

Submitted by:
SAHIL AHUJA
2K16/PIE/15

Under the supervision of

Dr. VIJAY GAUTAM
PROFESSOR

Dr. D S NAGESH
PROFESSOR

DEPARTMENT OF MECHANICAL, PRODUCTION &INDUSTRIAL AND AUTOMOBILE ENGINEERING,
DELHI TECHNOLOGICAL UNIVERSITY
(Formerly Delhi College of Engineering)
Bawana Road, Delhi-110042

DELHI TECHNOLOGICAL UNIVERSITY
(Formerly Delhi College of Engineering)
Bawana Road, Delhi-110042

CANDIDATE'S DECLARATION

I, SAHIL AHUJA, Roll No. 2K16/PIE/15, student of M.Tech (Production Engineering), hereby declare that the project Dissertation titled **"DESIGN AND ANALYSIS OF AN AUTOMOTIVE BRAKE DISC ON THE BASIS OF TEMPERATURE DISTRIBUTION"** which is submitted by me to the Department of Mechanical, Production & Industrial and Automobile engineering, Delhi Technological University, Delhi in partial fulfillment of the requirement for the award of the degree of Master of Technology, is original and not copied from any source without proper citation. This work has not previously formed the basis for the award of any Degree, Diploma Associateship, Fellowship or other similar title or recognition.

Place: Delhi
Date:

SAHIL AHUJA
2K16/PIE/15

DEPARTMENT OF MECHANICAL, PRODUCTION &INDUSTRIAL AND AUTOMOBILE ENGINEERING,
DELHI TECHNOLOGICAL UNIVERSITY
(Formerly Delhi College of Engineering)
Bawana Road, Delhi-110042

CERTIFICATE

We hereby certify that the Project Dissertation titled "**DESIGN AND ANALYSIS OF AN AUTOMOTIVE BRAKE DISC ON THE BASIS OF TEMPERATURE DISTRIBUTION"** which is submitted by Sahil Ahuja, Roll No. 2K16/PIE/15, Department of Mechanical, Production & Industrial and Automobile engineering, Delhi Technological University, Delhi in partial fulfillment of the requirement for the award of the degree of Master of Technology, is a record of the project work carried out by the student under our supervision. To the best of our knowledge this work has not been submitted in part or full for any Degree or Diploma to this university or elsewhere.

SUPERVISOR

Dr. VIJAY GAUTAM
PROFESSOR

SUPERVISOR

Dr. D S NAGESH
PROFESSOR

Place: Delhi
Date:

ACKNOWLEDGEMENT

It is a matter of great pleasure for me to present my dissertation report on "**DESIGN AND ANALYSIS OF AN AUTOMOTIVE BRAKE DISC ON THE BASIS OF TEMPERATURE DISTRIBUTION".** First and foremost, I am profoundly grateful to my guides **Dr. VIJAY GAUTAM, Professor,** and **Dr. DS NAGESH, Professor, Department of Mechanical Engineering** for their expert guidance and continuous encouragement during all stages of thesis. I feel lucky to get an opportunity to work with them. Not only their understanding toward the subject, but also their interpretation from the simulation help me think on a bigger way.

I am thankful to the kindness and generosity shown by them towards me, as it helped me morally to complete the project within time frame.

Place: Delhi
Date:

SAHIL AHUJA
2K16/PIE/15

ABSTRACT

Brakes are the most important safety feature of any vehicle. The current study deals with the temperature analysis of rotors made of different materials used in the front disc brake in APACHE RTR 160 motorbike under severe or hard braking conditions with single stop braking taking into assumption no slip (no locking of wheels) occurring at the tyre-ground interface. Single stop braking implies applying the brakes continuously from non-zero velocity till the velocity is reduced to zero. If the slip takes place between tyre and ground, then there is some loss of energy between them which will not be dissipated through the brake system. The materials chosen for the disc brake rotor are Grey Cast Iron, Ductile Cast Iron, Aluminium Metal Matrix Composite and Martensitic Stainless Steel. The model is developed using ABAQUS CAE and the dynamic temperature displacement explicit analysis has been performed. The simulation is performed and the results are compared analytically for the solid rotor. The temperature distribution obtained is utilized to find out the best material to be used as the disc material in the front disc considering cost, maximum temperature reached, mass of the disc, heat distribution, temperature distribution, hot spots, temperature gradients etc. Severe braking in emergency braking results in very high rise in temperature due to very short time span of braking resulting in higher braking power and high rate of heat generation with minimum amount of heat transfer taking place in surrounding due to convection and radiation in the braking phase. In the present work, heat transfer due to radiation is neglected.

Most of the braking power generated due to friction in severe braking is almost absorbed into the disc brake system. The thermal energy is mainly absorbed by the disc surface and pad surface in contact, and due to conduction it gets distributed to the pad, disc and to

components which are in contact with them. This also puts a need to verify whether the brake system material and different components would be able to bear such fast rise in temperature without failure.

The analysis is based on the energy conservation principle i.e. the energy possessed by the vehicle during the start of braking phase must almost be (taking 97%) absorbed in the disc brake system in the severe braking conditions with minimum heat loss taking place in surrounding due to very less time of braking. In the present work, total kinetic energy of the vehicle is provided as the rotational energy to the disc brake system using some design changes. This rotational energy is now dissipated in the form of heat energy due to real friction contact between the pad and the disc. The heat energy dissipated is distributed between the disc and the pad depending on the material properties of the disc and pad like mainly on thermal conductivity, density, specific heat and thermal diffusivity. In general, 90-95% of heat energy goes to the disc surface. The friction pad material has been kept same for different discs. It has been found out that the maximum temperature occurs in the frictional contact region of the disc and pad. The temperature is higher on the surface of the disc as compared to the inner portions. On the surface of frictional contact region of disc, the temperature increases to a maximum value and then decreases with braking time. Saw-tooth variation of temperature with respect to time is observed in the contact region nodes which is similar to the experimental results.

KEYWORDS: Disc brake, thermal analysis, energy conservation principle, ABAQUS

TABLE OF CONTENTS

LIST OF FIGURES

LIST OF TABLES

LIST OF SYMBOLS, ABBREVIATIONS, AND NOMENCLATURE

P_f	Braking power
K	Thermal conductivity
C	Specific heat
p	Density
E	Young's modulus
μ	Poisson's ratio
α	Coefficient of thermal expansion
λ	Thermal diffusivity
v/s	Versus
DTV	Disc thickness variation
DCI	Ductile cast iron
GCI	Grey cast iron
ALMMC	Aluminium metal matrix composite
MSS	Martensitic Stainless steel
NT	Nodal temperature

CHAPTER 1

INTRODUCTION

1. 1 INTRODUCTION OF DISC BRAKES

Brake system of automobiles is an important part of the safety feature. Brakes help in controlling the speed of the vehicle, either slowing down or stopping within a safe distance to provide both safety and control. There are many types of brakes based on their operating mechanism like pneumatic brakes, mechanical brakes, magnetic brakes, etc. Mechanical brakes work by converting the kinetic and potential energy possessed by the vehicle into thermal energy and dissipating it to the surrounding. Due to braking, friction forces are developed which opposes the relative motion between the stationary part, i.e., the brake pads and the rotating part, i.e., the disc or the drum. In braking, kinetic friction comes into play as the relative motion is there between the pads and the disc. Kinetic friction is a non-conservative friction resulting in generation of heat.

With the advancement of the transportation system, braking systems have also evolved a lot. Disc brakes are one of the mechanical brakes mostly in use today. Disc brakes are known for their ease of application, ease of maintenance, reliability, better time response, better cooling and their ability to with-stand higher temperatures than the drum brakes. Disc brake operated by hydraulic means consists of a rotor or disc, caliper, brake pads, master and slave cylinders, brake fluid, rubber sealing rings, hoses, etc. Hydraulic fluid provides better control as compared to the mechanical means. The diagram of a disc brake is given in Fig. 1.1. Rotor or disc is attached to the wheels through some protrusions from the hub with the help of bolts and rotates with the wheel. Caliper is a housing connected to a stationary part of the vehicle like suspension carrier, stub axle or axle casing [1]. The caliper is divided in two parts with each part having piston-cylinder arrangement operated hydraulically. Caliper is made of aluminium alloy to decrease the mass and must be very rigidly attached for better braking efficiency. The friction pad is held in between the pistons and the disc with the help of retaining pins, spring plates, etc. Brake pad consists of friction material and back plate generally made of steel. Brake pads

are made of low thermal conductivity to prevent the vaporization of brake fluids. Passages for the movement of brake fluids are provided in the caliper. Master cylinder is the brake fluid reservoir which is connected to the lever of the brake. In motorbikes, master cylinder is placed near the handle connected with the brake lever. On applying the brakes, the brake fluid is pressurized in the master cylinder. Hoses transfer the pressurized brake fluid to various parts of the disc brake. Slave cylinders are contained in the caliper portion and operated by fluid pressure and are an integral part of the caliper.

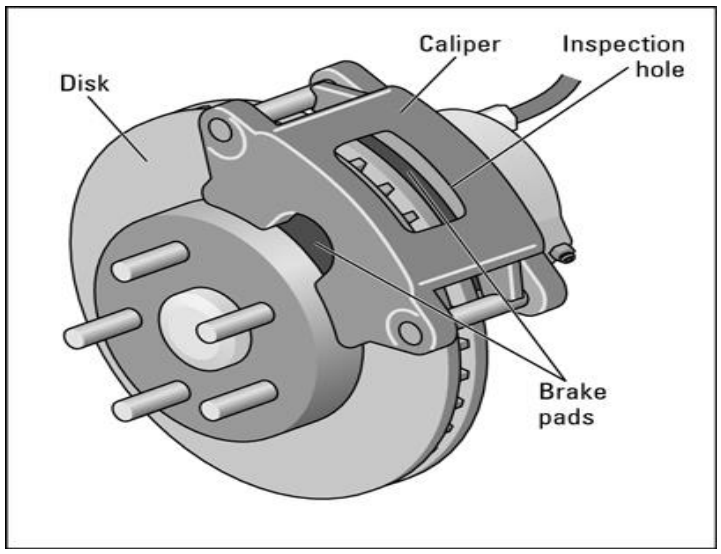

Fig. 1.1 Parts of a disc brake [2]

When the brakes are applied, the brake fluid is pressurized to move from the master cylinder to the slave cylinder through the hoses and pushes the pistons of the slave cylinder. The pistons of the slave cylinder move the friction pads axially into contact with the disc retarding the motion of the vehicle. A large amount of heat is generated due to the frictional forces developed between the disc and pads which leads to the rise in temperature of the rotor as well as pads. Depending on the material properties of the disc and pad, heat energy is distributed. In general cases, 90-95% of the heat energy is absorbed by the brake disc surfaces [3]. The material must, therefore, be chosen seeing the limits of maximum temperature that can be developed depending on the weight of the vehicle, maximum speed, fluid pressure, thermal properties of the materials, etc. In the present study of numerical analysis, the dynamic temperature displacement explicit analysis has been performed because both the thermal and structural properties are

dependent on one another at the same time. Thermals stresses and strains are dependent on the temperature and also temperature is dependent upon the stresses, strains, etc. But the influence of thermal behavior is considerable, hence the thermal behavior therefore needs to be investigated for the disc brake system. Excessive thermal loading and temperatures leads to brake fade (reduction in coefficient of friction), higher disc thickness variation (DTV), etc. On releasing the brake lever, hydraulic pressure collapses and the distorted rubber sealing act as return springs, thereby releasing the pressure on pistons and friction pad, removing contact between pad and disc. At braking, the major heat transfer mechanism is initially conduction through the brake disc and the pads. Gradually, with longer periods of braking, the temperature in the disc increases, heat is conducted to surrounding parts and cooling increases by convection and radiation [4]. The brake system must be designed in such a way as to maximise the heat transfer to the surroundings.

The major factors which determine the brake power of the system are the mass of the vehicle, the speed of the vehicle, stopping distance and deceleration rate, the pressure applied on brake pads, the coefficient of friction between disc and pads, initial brake temperature, environmental conditions (ambient temperature and wind) and tyre-ground contact conditions. To identify the safety and braking capacity, testing of brakes is done in different ways matching the conditions during actual running. All the tests are important as all are focusing on different criteria and therefore different conclusions can be drawn from the results. For the testing purpose of the brakes, three different types of braking conditions can be defined. These conditions are generally followed when a vehicle is driven. The first is “stop braking” where the speed of the vehicle is reduced until stop. In this type, brakes are applied continuously until the vehicle is brought to rest. This type of braking is relatively rare and may sometimes be used in accidental conditions, but it is important concerning the thermal analysis as the temperature rises very rapidly. The main characteristic of single stop braking is that braking times are relatively small, implying that heat is mostly absorbed by the brake system and heat dissipation is quite low and can be neglected. The role of convection and radiation is negligible during brake applications. In the present study, single stop braking condition is simulated including convection. The second is “normal braking” or “repeated braking”,

also known as “stub braking”, where the speed is decreased as required for safety reasons like keeping the distance between vehicles or changes in speed limits. In this type the brakes are not applied continuously for stopping the vehicle. Rather the main purpose is speed control. In this, braking is applied at relatively close intervals. From the thermal point of view, each brake application results in small heat generation, but successive brake applications build up a substantial amount of heat energy which needs to be dissipated, so brake cooling is required in these events. Convection and radiation play an important role in cooling. Brake fade analysis is the main criteria in the stub braking test. The third one is “drag braking”, also referred to as “downhill braking”, in which the brakes are used for maintaining speed when traveling down a gradient. Hence in this as the vehicle moves down a slope, the speed is kept constant with the help of braking. In this type, the potential energy of the vehicle keeps on decreasing during downhill motion, and this potential energy is converted to heat to keep the vehicle running at a constant speed [4]. This type of braking is almost continuous but here the vehicle is made to run at constant speed. From thermal point of view, due to higher time of application of brakes, the heat generation is very high.

In the present study, “single stop” braking is used for the numerical analysis where the brakes are applied to the vehicle with initial translational velocity of 15m/s (angular velocity of 67.5rad/s) till the vehicle is brought to a complete stop in 1.6 s. Since the braking time is relatively small the role of convection as well as radiation will be negligible. In this work, convection is included in the analysis and radiation has been neglected.

1.2 TYPES OF DISC BRAKES

Disc brakes are of different types depending on the geometry, construction, calipers, position of calipers, number of calipers, etc. The type used depends on the application, braking power, material, vehicle design, etc. There are three types of disc brakes based on the type of calipers which are fixed caliper disc brake, floating caliper disc brake, and sliding caliper disc brake.

Fixed Caliper Disc Brake

In fixed caliper disc brake, the caliper doesn't change its position concerning the disc. Caliper is fixed and only there is motion of pistons and pads. A fixed caliper has pistons on both sides of the disc as shown in Fig.1.2. Hydraulic pressure lines are present on both sides of the caliper to pressurise the pads. Usually, two pistons are used, one on each side. Some use four to six pistons with two and three on each side respectively. The caliper is rigidly attached to the stationary part of the vehicle like steering knuckle, stub axle, axle casing, suspension carrier, etc. In this, only the pistons and pads move when the brakes are applied. The pad wear in fixed- caliper disc is more balanced and uniform than the floating and sliding caliper disc brake. The cost of this system is highest owing to the more number of hydraulic lines on both sides. The design is more robust and has higher and more uniform braking effect. In high end and high speed vehicles, this system is preferred. In the present study, the fixed caliper disc brake system is selected for the numerical analysis.

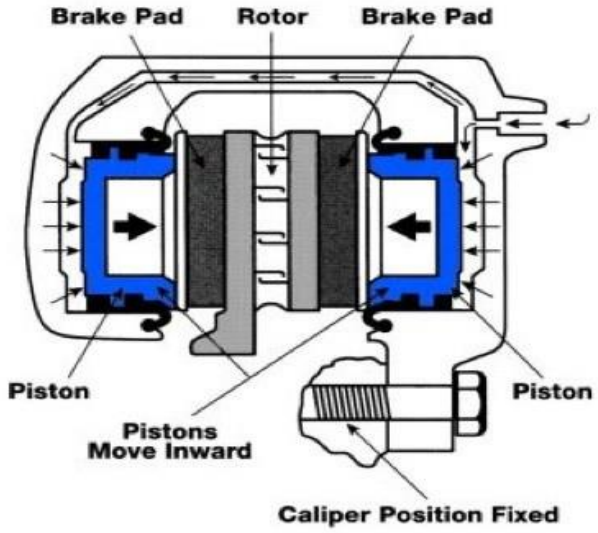

Fig. 1.2 Fixed caliper disc brake [5]

Floating Caliper Disc Brake

In floating caliper disc brake, the caliper swings or floats during braking about a pin. It has pistons located only on one side (inboard side) of the disc. The hydraulic line coming from the master cylinder enters only one side of the caliper. So the pressure is applied

only on one side of disc surface on the pad. These are the most commonly used disc brake in two wheelers. The caliper is hinged about a fulcrum pin, and one of the friction pads is fixed to the caliper as shown in Fig. 1.3. The motion of friction pad is controlled by the movement of the caliper. The fluid under pressure presses the inboard pad against the disc to apply the brake. The reaction on the caliper causes it to move the fixed pad inward slightly, applying equal pressure to the other side of the disc. The caliper automatically adjusts its position by swinging about the pin. Floating calipers offers a number of advantages over fixed-caliper designs [6]. They have a lower brake fluid operating temperature and hence lower potential for brake fluid vaporization, but the braking effect is lower as compared to fixed case. There is more wear on one brake pad as compared to the other. Cost of the floating-caliper system is less as compared to the fixed-caliper system.

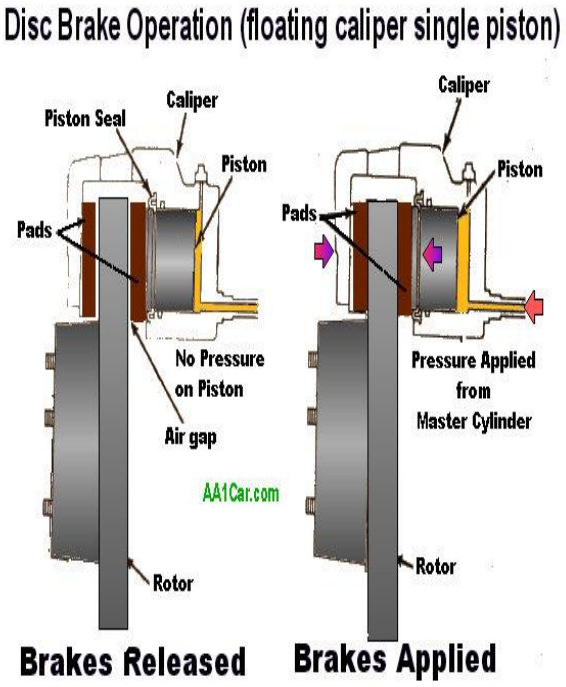

Fig. 1.3 Floating caliper disc brake [7]

Sliding Caliper Disc Brake

In this, the caliper slides on machined surfaces on the steering knuckle adapter or anchor plate, and no guide pins are used in this. One of the friction pads is fixed to the caliper just like the floating caliper brake, and other pad is pressurized through the fluid. So the

other pad is pressed indirectly by the caliper as shown in Fig. 1.4. This system is used in APACHE RTR 160 motorbike.

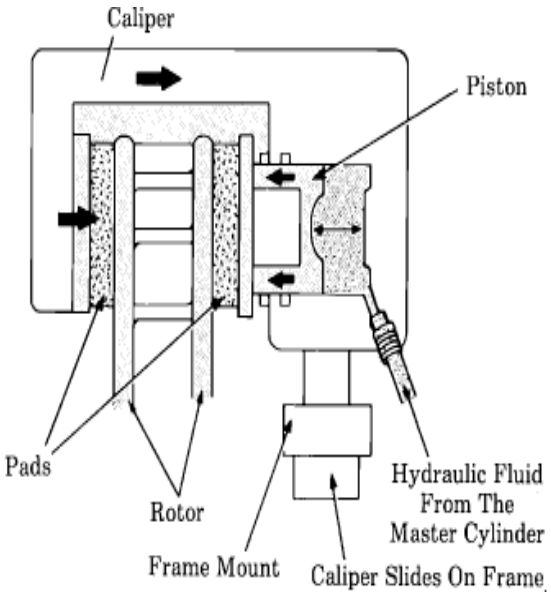

Fig. 1.4 Sliding caliper disc brake [8]

1.3 WEIGHT TRANSFER DURING BRAKING

The main function of braking is to reduce the speed of the vehicle. Braking depends on the coefficient of friction between the tyre and ground interface. This coefficient of friction is dependent on tyre and road conditions, the normal reaction force and the speed. The most common dynamic effect of braking observed is the 'dive' where the nose of the vehicle dips because of weight transfer. During braking, it has been observed that the vehicle bends in the forward direction. The Fig. 1.5 below shows the various forces acting at the time of application of brakes to a moving vehicle. The inertia force acts at the center of gravity of the vehicle, while the retarding force due to the application of brakes acts at the road surface. As a result, these two forces form a couple. This couple increases the perpendicular force between front wheels and the ground, while the perpendicular force between the rear wheels and the ground is decreased by an equal amount [1]. The result is a transfer of some of the vehicle weight to the front axle from

the rear axle. Therefore, higher braking effort should be applied at the front wheels for efficient braking. It is seen that in general for achieving maximum efficiency, about 70-75% of the braking should be on the front wheels. If the braking effort is put more on the rear disc, then there is a great possibility of wheels locking up and loosing of drive control.

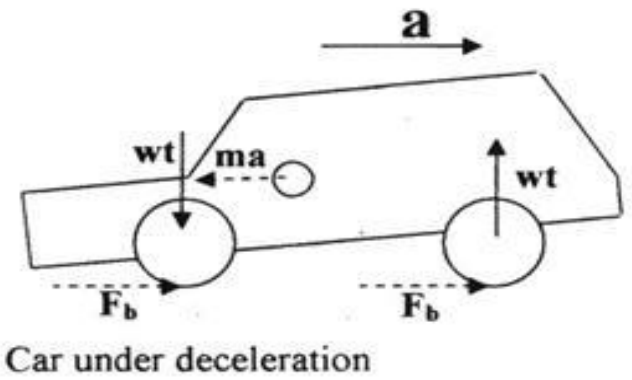

Fig. 1.5 FBD of weight transfer on front axle during braking [9]

1.4 PAD PRESSURE AND WEAR IN DISC BRAKES

Wear distribution and pad contact with the disc must be uniform. To maintain uniform contact over the pads, the pressure applied by the caliper must also be uniform. Uniform pressure between the pad and rotor results in uniform pad wear distribution and brake temperature. Non- uniform pressure distribution cause uneven wear of the pads. Worn or old disc pads may show significantly higher wear on the leading end (rotor entrance) as compared to the trailing end (rotor exit). This non-uniform wear is caused by higher pressure between the pad and the rotor at the leading end as compared to the trailing end. The non-uniform pressure distribution is caused by the moment generated between pad drag force and abutment force (pad stopping force). This moment cause the pads to press with higher pressure on the leading end as compared to the trailing end. As a result, leading ends are worn more as compared to trailing ends. For a symmetrical wheel cylinder piston and pad design, the drag/abutment force moment results in pad pressures

at the leading end that are approximately one-third greater than the average pressure. The corresponding pressure at the trailing end is approximately two-thirds of average pad pressure [4].

To overcome this problem of minimizing or eliminating tapered pad wear involve an off-center pad application force produced by an asymmetrical caliper piston contact edge, effectively moving the piston force in the direction of the trailing end of the pad, which creates a counter moment balancing the pad friction moment [4].

Other solutions include locating the piston closer to the trailing end of the pad, again producing a counter moment. Expensive designs minimizing tapered pad wear use four pistons per caliper. The pads are pushed with two pistons of different diameter, with the smaller piston located at the leading end of the pad.

1.5 DISC OR ROTOR

Rotors, also called brake discs, are mounted to the hub and rotate with the wheel and tyre. The center of the rotor, called the hat, provides the mounting point for the rotor on the hub. The center hub hole is designed to fit precisely to the hub. A large amount of friction is created between the pads and rotor due to the clamping of brake pads against the rotor. This friction is what slows the wheel and generates intense heat. Because of the stresses of braking and the heat that is generated, brake rotors must be strong and able to withstand high operating temperatures. Both Mechanical and thermal stresses are generated due to the heating and mechanical loading. Also local overheating or hot spots in brake disc resulting from frictional heat may lead to changes in material structure, cracks, and damages shortening its lifespan. The most common brake rotors are made of cast iron. The material is cheap and has good anti-fade properties [10]. Two types of rotor have been employed in making of disc brakes, i.e., the solid and vented type. The type of rotor pictured in Fig. 1.6, is called a vented rotor. The vents are located between the two friction surfaces. The overall friction surface area is large, but the contact area of the pads is small. As the pads are pressed against the rotor, heat is generated all around the rotor's surfaces. The front brake rotors on all modern cars, trucks are vented.

Fig. 1.6 Vented rotor

Fig. 1.7 Solid rotor

Non-vented or solid rotors, like the rotor in the Fig. 1.7, are used on the rear of some vehicles, and they can be found on the front of some older, smaller vehicles. Non-vented rotors can be used in the rear since the rear brakes are doing less work than the front brakes, and the additional cooling is not necessary. The ventilated rotors provide better cooling efficiency, but the rise in temperature is faster in ventilated rotors due to some amount of material removal to make the vents. To overcome this, ventilated discs are made thicker and a little bit heavier than solid discs. For many vehicles, the vents in the rotors are simply straight passages from the outside to the inside of the hub or hat section of the rotor. Some vehicles use rotors that have curved or directional vents. Rotors with directional vents have improved airflow for better heat dissipation, but they must be installed on the correct side of the vehicle to work correctly.

For efficient functioning of the disc brake, the rotor material should possess the following properties:

1- High, uniform, and stable coefficient of friction.

2- Inertness to environmental conditions.

3- Ability to withstand high temperature (thermal stability).

4- High wear resistance.

5- Flexibility and conformability to any surface.

6- Good thermal conductivity and heat absorption capacity.

7- High strength and durability to sustain torque loads.
8- High vibration damping capacities to minimize the problem of squeal and judder.

The dynamic or sliding coefficient of friction between the rotor and pads needs to be stable for braking efficiency. Different combination of the disc and the pad material provide different values of coefficient of friction. Various materials used for rotor are mentioned below:

GREY CAST IRON (GCI)

Cast iron is the class of iron based alloys containing more than 2% but less than 4.3% carbon. These are ternary alloys comprising mainly of iron, with specific values of carbon and silicon which have a significant effect on the structure, type and the matrix developed. Matrix, grain size and structure are further influenced by the heat treatment, other alloying elements, casting process, etc. Carbon equivalent (CE) is generally used for the specification of different types of cast iron. It is the summation of the percentage of carbon and one-third percentage of Silicon (sometime phosphorous percentage is also included). The maximum amount of carbon that can be dissolved in a single phase is 2% [11]. The excess carbon result in heterogeneous nature of cast iron alloys.

$$CE = \%C + \frac{\%Si}{3} \tag{1.1}$$

Grey iron is a special class of cast iron. It is also called as the flake or lamellar graphite cast iron due to the solidification of graphite in the form of randomly distributed flakes as shown in Fig. 1.8. Graphite flakes influence the properties of the grey iron. Fracture of grey iron occurs on the fracture path following the graphite flakes, resulting in the characteristic grey color of the fracture and giving rise to the name of this family of cast iron alloys. The size, shape, distribution and amount of the graphite flakes have an important contribution in the properties of grey iron. The type of matrix, i.e., ferritic, pearlitic, or a mixture of both, size of the graphite flakes and distribution of flakes also influence the hardness and properties. The percentage of ferrite and pearlite also influence the properties. These characteristics are determined by both the composition of the raw materials (primarily by the amount of carbon and silicon) and by the cooling rates

(during both solidification and solid state). Slower cooling rates result in higher ferrite portion providing more softness, ductility and less hardness. Higher carbon and silicon percentage result in more and larger graphite flakes, a softer matrix, and lower strength. Low values of silicon result in most of the carbon forming cementite which is a very hard compound. Fast cooling rates and the addition of some alloying elements like vanadium, molybdenum, carbide formers, etc. result in a harder matrix with higher strength [11].

The presence of graphite flakes provides grey iron with unique mechanical properties (example excellent machinability at hardness values that produce superior wear resistance, excellent damping characteristics attributed to the flake graphite morphology as well as a nonlinear stress-strain relationship at low stresses, resistance to galling), physical properties (thermal conductivity), and casting characteristics (superior castability, reduced shrinkage, etc) [11]. Of all the cast irons, grey iron has the lowest melting temperatures.

The casting of grey iron is better in induction furnaces because of reduction in oxidation losses during melting and elimination of coke as the fuel. In induction furnace, the composition of charge material almost completely defines the composition of cast. Hence accurate charge calculations are required to provide better control of the composition. The grey iron is made by melting of steel scrap, cast iron scrap and using ferrosilicon as the inoculant.

Fig. 1.8 Microstructure of grey cast iron [12]

It is the most common material used in disc brake rotors. Grey iron is named because its fracture surface has a gray appearance and it consists of carbon in the form of flake graphite in a matrix consisting of ferrite, pearlite or a mixture of the two [13]. It provides good wear resistance, good castability, moderate strength, high thermal conductivity, low

cost and excellent vibration damping properties but the main drawback is the high density which results in a higher weight of the disc. Grey cast iron also maintain their mechanical properties up to approximately 500^{o}C, above which the mechanical properties decrease significantly.

DUCTILE CAST IRON (DCI)

Ductile iron is also a type of cast iron. Ductile iron is also known as nodular or spheroidal graphite iron. The roughly spherical shape of nodules is the characteristic feature of all the Ductile Iron. The shape, size, distribution and density of these nodules have significant effect on the material properties. As shown in Fig.1.9, these nodules act as "crack-arresters" and make Ductile Iron "ductile" [14]. The formation of nodules is achieved by the addition of nodularizing elements, most commonly magnesium (sometimes cerium). Ductile iron has a unique combination of a wide range of properties like ductility, high strength, wear resistance, fatigue resistance, and toughness in addition to the known advantages of cast iron like castability, machinability, damping capacity, etc.

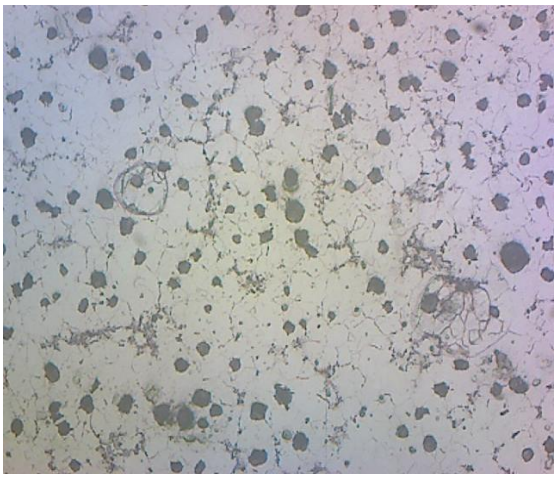

Fig. 1.9 Microstructure of ductile cast iron

Ductile Iron is a family of materials offering a wide range of properties obtained through microstructure control by varying the composition of initial raw materials, heat treatment, casting process control, etc. It is made by treating low sulphur molten liquid metal with magnesium (sometimes cerium) as the nodularizing agent and is inoculated with silicon

containing alloys like ferrosilicon during the casting. The sulphur content of the molten metal should be kept lower (<0.02%). This is achieved by using high quality pig iron. The base iron composition must be carefully controlled to prevent the introduction of certain minor elements that interfere with nodules formation. The temperatures are set at around 1400^{o}C. The nodular form of graphite is achieved with a magnesium content of 0.04%-0.06%. Magnesium is a highly reactive element at 1400^{o}C and combines readily with oxygen and sulphur. Hence, magnesium treatment should be done very carefully else it might cause injuries. The raw materials used are steel scrap, pig iron, ferrosilicon to form a molten liquid metal. Treatment to produce ductile iron involves the addition of magnesium to change the morphological form of the graphite, followed by or combined with inoculation of a silicon-containing material to ensure a graphitic structure with freedom from Carbides. In one of the treatment way, magnesium powder is kept at the bottom of the crucible for the magnesium treatment. After magnesium layer of metal, it is covered with a sheet steel so as to prevent violent reaction of magnesium at higher temperatures. When this method is used, the alloy is often placed into a specially designed pocket and covered with a layer of steel turnings (this is known as the sandwich process). The use of a cover with a tundish through which the iron can be poured reduces any ejection of metal, fume, and flame and improves the yield of magnesium. Above this ferrosilicon powder is kept for inoculation purpose. The main advantage of this material is high strength, wear resistance, fatigue resistance, resistance to thermal fatigue, toughness and ductility in addition to the known advantages of cast iron like castability, machinability, damping property [13].

MARTENSITIC STAINLESS STEEL (MSS)

Stainless steels are alloy steels with a chromium content of atleast 11% (weight percent) with other additions. Martensitic Stainless steel forms very hard crystalline structure after hardening heat treatment of stainless steel. These steels have body-centred tetragonal (BCT) crystal structure. These steels undergo austenite to martensite transformation in almost all cooling conditions. Tempering further can result in softer martensitic, fully ferritic structure. Martensitic Stainless steel disc is generally used in 2 wheelers in the

current scenario. These steels have high oxidation resistance due to presence of a chromium rich oxide film on the surface

ALUMINIUM METAL MATRIX COMPOSITE (ALMMC)

Composites are always two-phase materials comprising of matrix phase and reinforcement phase. Matrix phase is a continuous phase and reinforcement phase is a discontinuous phase either in the form of particles, fibers, or whiskers [15]. The reinforcement phase is selected as the material with superior properties than the matrix phase. In the current work, particulate reinforced composite is considered which is generally made by stir casting technique. In this type of composite, the reinforcement phase is in the form of particles dispersed in the molten matrix phase.

Aluminium is a very light metal with a low density of around 2700kg/m^3. It has good thermal conductivity, corrosion resistance, less density, high ductility and it is highly recyclable. Silica (silicon dioxide, SiO_2) is a compound of silicon and carbon. It has high strength, high hardness, high wear resistance, low thermal expansion coefficient, low density, superior chemical inertness, etc. Aluminium metal matrix composite with silica particulate combines the advantages of aluminium and silica [16]. The addition of high strength and high hardness silica particles to a ductile metal produces properties intermediate of both of the phases. In stir casting technique, dispersed phase is put in the molten liquid metal. To provide good mechanical properties to the composite, good bonding (wetting) between both the phases should take place. The dispersed phase is mixed with the molten matrix by means of mechanical stirring. The liquid composite material is then cast as a general casting in the designed mould.

Aluminium alloy is melted in a crucible by heating it upto 850^{o}C in a furnace for around 3 hours in stir casting machine [17]. The silica particles are preheated at around 600^{o}C in a muffle furnace. The stir casting machine furnace temperature is used to raise the temperature above the liquidus temperature of aluminium alloy to around 850^{o}C to melt completely and then cooled a bit to keep it in the form of a semi-solid slurry. Stirring is carried out continuously for around 5 minutes, and then the preheated silica particles were dispersed in the molten liquid. The furnace temperature was controlled at around

750^{o}C for around 30 minutes. After uniform mixing of the particles in molten slurry, the mixture was poured in the mould cavity.

Aluminium metal matrix composites with ceramic particulate reinforcement are known for their low density, high thermal conductivity, corrosion resistance, etc. The low density makes the weight of the rotor very less. The reinforcement in the ALMMC could be in the form of continuous or discontinuous fibers, whiskers, precipitates. They have nowadays gained more importance in aerospace, defence and automotive areas.

While being much lighter than cast iron they are not as resistant to higher temperatures and in general used mostly in the rear disc brake since the braking efforts are less in the rear axle.

1.6 BRAKE PAD OVERVIEW

Brake pads are one of the most important components in the braking system. The brake pads are made of low thermal conductivity, highly insulating material so as to absorb most of the heat produced during braking and only a small portion of heat is conducted through it back to the piston to prevent the vaporization of brake fluid. Brake pads convert the kinetic and potential energy possessed by the vehicle into heat energy using frictional contact with the rotor which must be dissipated. In general, brake pads are manufactured using powder metallurgy. To achieve the wide range of properties required by brakes, brake materials are composites made of a large number of elements, rather than a single element. They consist of friction materials, backing plate and wear indicator. The backing plate is usually fabricated from low-carbon steels. The function of the backing plates is to transmit the force from the caliper pistons to the friction material. It may also contain retention features such as holes or serrated edges to provide a better anchor point for the friction material [18]. Wear out of the pads is inevitable with time. Wear indicators are used to inform the driver of the need of the replacement. In most cases a simple steel spring is riveted to the brake pad backing plate to serve this purpose. When the friction material wears to the point that replacement is necessary, the spring

will contact the rotor, emitting a high-pitched squeal. Nowadays wear indicators are made as a cut in the pad itself and also serve the purpose of removing dust, foreign particles, etc. which might get stuck in between the pad and the disc due to wear-out and surroundings. In the present study, three wear indicators are modeled in the pads based on the real manufacturing of the pads as shown in Fig. 1.10.

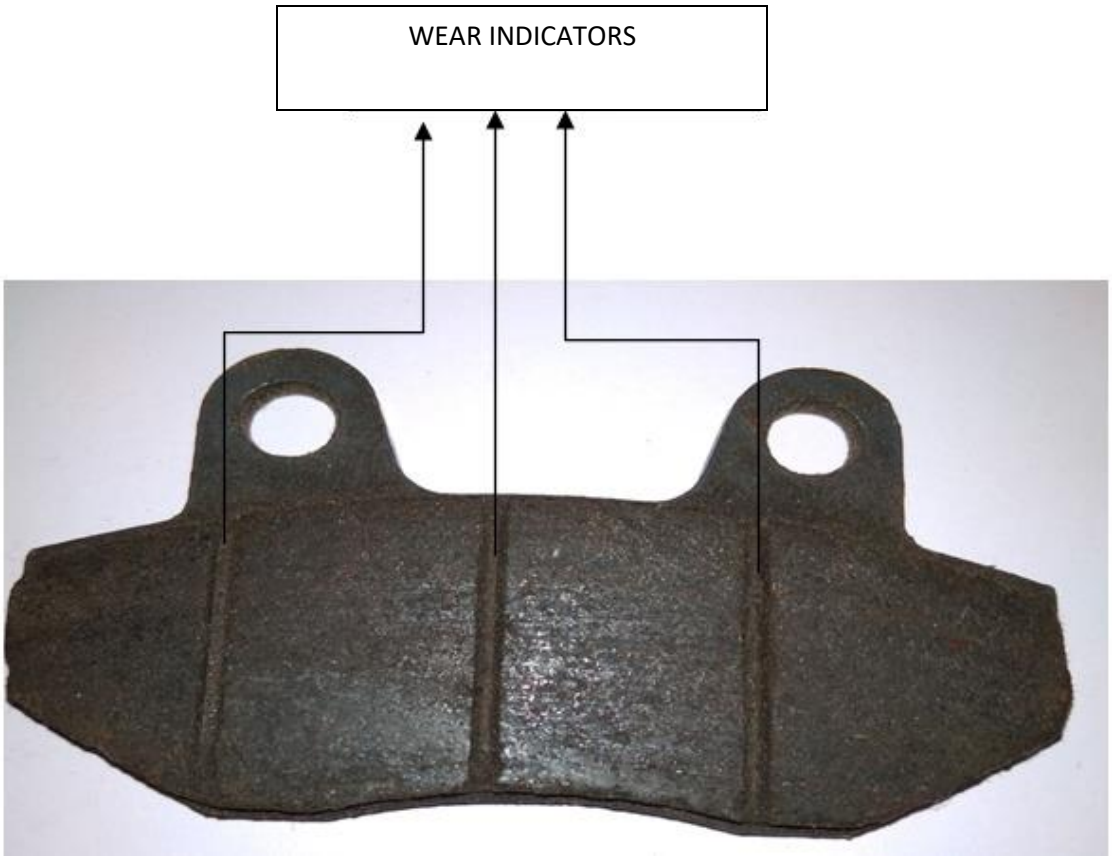

Fig. 1.10 Pad used in motorbike with wear indicators

Of all the materials in the brake pads, the friction material is arguably the most critical from a high performance perspective. Friction materials are made using a mixture of materials. In general, friction materials are composed of four subcomponents: abrasives, friction modifiers, fillers and reinforcements, and binder materials. Abrasives provide the required friction depending on the application and control the build-up of friction films. Various examples of abrasives used are aluminum oxide, iron oxides, quartz, silica and zirconium silicate. Chemical composition, distribution, form and particle size of the abrasive have great influence on the friction between the contacting areas. Friction modifies lubricate, or raise the friction to help control the interfacial films. Various

friction modifiers used are brass, graphite, lead oxide, etc. Fillers are used to maintain the overall composition of friction material, these can be metals, alloys, ceramics or organic materials. Various fillers used are asbestos, barium sulphate, cashew nut shell oil, cotton, rubber scrap, zinc oxide, etc. Cashew containing friction dust is said to have the ability to absorb the heat created by friction while retaining braking efficiency. Binders are typically phenolic resins in case of automotive pads. Reinforcing fibers provide mechanical strength. The brake pads are designed for high friction values. Binder materials are used to hold different materials together and prevent disintegration [19]. Earlier most of the pads were made using asbestos but due to environmental issues use of asbestos has been banned.

1.6.1 FRICTION MATERIALS

The friction materials generally used are:

ASBESTOS

Asbestos is hydrated magnesium silicate $Mg_3Si_20_5(OH)_4$. Asbestos was the best choice of material in the manufacture of brake pads in past. This is because of its good properties such as ability to withstand high temperatures, strong yet flexible, wears well, available at reasonable cost which are essential in brake pads. Asbestos was also readily available. However, in the early 1980s it was discovered to be carcinogenic and was capable of causing Asbestosis and Mesothelioma.

SEMI-METALLIC

Semi-metallic pads consist of high amount of metallic portion ranging upto 40 percent and other ingredients which include fillers, binders and lubricants. Carbon based semi-metallic pads are also a reality now. Semi-metallic pads are strong, conduct more heat away from rotors due to more metallic content, generate more noise and are more rough to increase rotor wear. They have low to medium coefficient of friction ranging 0.28 – 0.38.

METALLIC PADS

Metallic pads are typically made of iron, copper, steel and graphite all mixed together and bonded to form the pad material. The pads are cost-effective and durable. They are also good at transferring the heat generated by friction with the brake rotors .However, being made of metal, the pads are very hard. This makes them to cause more wear on the brake rotors. They do not work well when cold, they are noisy and dust resistant.

CERAMIC PADS

Ceramics pads are made of ceramics compounds which have a composition of about 15 percent metal fibers and other ingredients such as fillers, binders, and lubricants. The various fillers and lubricants help dampen vibration and noise and hence these pads are quiet in operation [17]. These pads wear less, transfer heat better because of metal fibers and are lighter in weight**.** These pads are used in high speed racing cars along with carbon fiber disc. These materials are very costly and are normally not used in moderate cost vehicles. The materials that make up the pad friction material determine its coefficient of friction and ultimately, how well the vehicle stops. Common ingredients include iron, steel, copper, synthetic fibers, and ceramics. The pads must be made from materials that can not only withstand the friction and heat of braking, but also be able to operate effectively when the brakes are cold. Brake pad linings are a compromise between several factors, such as pad life, noise generation, and cold and hot coefficients of friction.

1.7 THERMAL ANALYSIS

Heat generation and brake temperature is a combined result of velocity of vehicle, pad pressure, coefficient of friction between disc and pad, tyre-ground contact conditions and weight of the vehicle. The coefficient of friction depends upon the applied pressure, surface conditions of the pad and disc, and material properties [4]. Brakes must be designed such that the operating temperatures are kept below the safe limit of individual brake components including pad, rotor, brake fluid, calipers, wheel cylinders, and seals.

1.7.1 BRAKING ENERGY AND POWER

For a vehicle decelerating on a flat surface from higher velocity V_1 to a lower velocity V_2, the braking energy E_f is

$$E_f = \frac{m\,(V_1^2 - V_2^2)}{2} + \frac{I\,(\omega_1^2 - \omega_2^2)}{2} \quad (1.2)$$

Where, I= mass moment of inertia of rotating parts

m=mass of the vehicle

V_1= initial velocity

V_2= final velocity

ω_1 =initial angular velocity

ω_2 = final angular velocity

If the vehicle comes to a complete stop, then $V_2 = \omega_2 = 0$ and Eq. (1.2) becomes

$$E_f = \frac{m\,(V_1^2)}{2} + \frac{I\,(\omega_1^2)}{2} \quad (1.3)$$

We know that $V = \omega R$

Where, R=radius of the wheel, therefore Eq. (1.3) becomes

$$E_f = \frac{m}{2}\left(1 + \frac{I}{R^2 m}\right) V_1^{2} = \frac{KmV_1^2}{2} \quad (1.4)$$

Where, k =correction factor for rotating masses

Typical values of K for motorbike range from 1.05-1.11 in high gear.

Braking power P_f is equal to the rate of change of braking energy with respect to time t during which braking occurs, or

$$P_f = \frac{d(E)}{dt} \quad (1.5)$$

If the deceleration "a" is constant, then the velocity $V(t)$ is given by

$$V(t) = V_1 - at \quad (1.6)$$

Where, a=deceleration

t=time

Eq. (1.5) gives the instantaneous brake power using Eq. (1.6) as

$$P_f = Kma(V_1 - at) \quad (1.7)$$

From Eq. (1.7) we can conclude that the braking power is maximum when t=0 and is minimum when the vehicle stops. Therefore, the braking power varies with time during the braking phase, being maximum at the start of braking, further decreasing and finally becoming zero.

Let the time for the vehicle to be stopped is t_s

$$t_s = \frac{V_1}{a} \quad (1.8)$$

The average braking power P_{fav}, over the braking time t_s for a vehicle coming to a stop is

$$P_{fav} = \frac{K\ m\ a\ V_1}{2} \quad (1.9)$$

1.8 INFLUENCE OF THERMAL PROPERTIES

Six properties are included in the material definitions which include thermal conductivity (K), Specific heat (C), density (ρ), Young's modulus (E), Poisson's ratio (μ) and coefficient of thermal expansion (α). Three of the above properties play an important role in the temperature distribution. These are thermal conductivity (K), Specific heat (C), and density (ρ).

Specific heat (C) - It is defined as the energy required to raise the temperature of unit mass of the substance by unit degree. This property has its significance in the static condition when temperature is independent of position and time. The units of specific heat are J/kg-K.

Thermal conductivity (K) - Conduction in metals is on account of lattice vibrations and free electron transfer. This conduction is related to the thermo-physical property of the material known as thermal conductivity. Thermal conductivity is defined as the rate of heat transfer through unit thickness of the material per unit area per unit temperature difference. Thermal conductivity has major significance in steady state problems when the temperature doesn't vary with time. Its unit is W/m-K.

Thermal diffusivity (λ) - It is a parameter which is a combination of thermal conductivity, specific heat and density. It is defined as the ratio of thermal conductivity to the product of specific heat and density as

$$\lambda = \frac{K}{pC} \tag{1.10}$$

Thermal diffusivity is a ratio between the thermal conductivity and volumetric heat storage capacity. It provides the information about the completion between the heat storage and conduction. It is a measure of thermal inertia and tells about the rate which the heat generated diffuses out of the material. This ratio is most important during transient heat transfer conduction as is the case of disc brake analysis. The larger the thermal diffusivity, the faster the heat propagates into the medium. A small value of λ means that heat is mostly absorbed by the material and a small amount is conducted further [20].

1.9 CONVECTION HEAT TRANSFER COEFFICIENT

The computation of brake temperature requires information on the convective heat transfer coefficient, which varies with vehicle speed, design and position of the brake components. In many cases it is sufficient to evaluate the heat transfer coefficient at some mean speed. Also the brakes are cooled by conduction and radiation. But conduction only redistributes heat, and thus, temperature and, and may affect other critical components in an unsafe manner such as bearing, lubricants, or seals.

It is necessary to state that any formula expressing heat transfer coefficient will yield only approximate results [4]. An expression showing the cooling is:

$$Nu=CRe^{m}Pr^{n} \quad (1.11)$$

Where, C=Heat transfer constant

Nu=Nusselt number=$\frac{h_R D_{out}}{K_a}$

h_R= Convection heat transfer coefficient

D_{out}=Outer diameter of disc

K_a=Thermal conductivity of air

Re= Reynolds number= $\frac{p_a V D_{out}}{\mu_a}$

$p_{a=}$ Density of air

V= Vehicle speed

μ_a= Kinematic viscosity of air

Pr= Prandtl number=$\frac{3600\, c_a m_a}{K_a}$

c_a = Specific heat of air

m_a = Mass flow rate of air

m,n= Heat transfer parameter constants

The constant C is a function of the geometry of the brake and has different values for brake drums, solid rotors, and ventilated rotors.

The heat transfer parameter m is a function of the type of flow, i.e. turbulent, laminar, or transitional flow. The heat transfer parameter n is a function of the properties of the flowing air.

1.10 CONVECTION HEAT TRANSFER COEFFICIENTS FOR SOLID DISCS

For solid, non- ventilated disc brake the convection heat transfer coefficient associated with laminar flow is approximated by [4]

$h_R = 0.7(\frac{K_a}{D_{out}})Re^{0.55}$ (for Re<$2.4*10^5$) (1.12)

In the present study, since for Re > $2.4x10^5$, the flow characteristics become turbulent and the convection heat transfer coefficient is approximated by

$h_R = 0.04(\frac{K_a}{D_{out}})Re^{0.8}$ (1.13)

1.11 ANALYTICAL METHOD FOR TEMPERATURE ANALYSIS

The solid non-ventilated rotor been considered in the analysis is subjected to cooling on both the surfaces and heated by the heat generated due to friction with the conduction taking place. For these conditions there is an analytical solution for temperature using constant heat flux as given below in Eq. 1.14 [4]:

$$\Theta_0(z,t) = \frac{q''_0}{h_R}[2(\frac{\Theta i\, hR}{q''_o}-1)\sum_{n=1}^{\infty} \frac{\sin(\lambda_n L)}{\lambda_n L+\cos(\lambda_n L)\sin(\lambda_n L)} e^{\wedge}(-a_t\lambda^2{}_n t)\cos(\lambda_n Z)+1] \quad (1.14)$$

Where, $a_t=\frac{K}{pC}$=thermal diffusivity

h_R=convective heat transfer coefficient

L = one-half rotor thickness

n = numbers 1, 2, 3

q_0" =average heat flux into rotor

t = time in hour

T_0 (z, t) =Transient temperature distribution in rotor due to constant heat flux

T_i= initial temperature

T_∞=ambient temperature

z = horizontal distance measured from mid-plane of rotor

$\Theta_0(z, t) = T_0(z, t)-T_\infty$= relative temperature of brake resulting from constant heat flux

$\Theta_i = T_i-T_a$=initial temperature difference between brake and ambient

$\lambda_n = n\Pi/L$

For braking times greater than 0.5 to 1 second, only first term (n=1) is sufficient in the summation for an acceptable accuracy of temperatures [4].

The above equation computes the temperature response from a constant heat flux at the rotor surface. But when the vehicle decelerates, the heat flux varies with time. Taking linearly decreasing heat flux, the temperature is obtained by using the above equation with the application of Duhamel theorem or superposition integral. This results in the final equation as Eq. 1.15:

$$\Theta(z,t)= \frac{q''_{(0)}}{q''_0} \times \Theta_0(z, \quad t) - \frac{q''_{(0)}}{t_s h_R}\left[t - 2\sum_{n=1}^{\infty} \frac{\sin(\lambda_n L)}{\lambda_n L + \cos(\lambda_n L)\sin(\lambda_n L)}\left(\frac{\cos(\lambda_n Z)}{a_t \lambda_n^2}\right) 1 - e^{\wedge}(-a_t \lambda^2{}_n \quad t)\right], \quad (1.15)$$

Where, $q''_{(0)}$=time-varying heat flux into one rotor surface at time t=0

q''_0 =average heat flux into rotor

t_s =braking time to stop in hour

CHAPTER 2

LITERATURE REVIEW

2.1 INTRODUCTION

A lot of research has been done on the disc brakes regarding the transient thermal analysis of brake pads and rotor. Most of the researchers have done the analysis on disc brake thermal analysis by calculating the kinetic energy from the mass of the vehicle and velocity, calculating heat flux from this energy and applying the heat flux on the rotor surface. Some researchers have also done the analysis by running the disc brake at constant speed for a predetermined amount of time with the brakes being pressed and then obtaining the temperatures.

2.2 RESEARCH REVIEW

A.Belhocine and M.Bouchetara [21] analyze the thermo-mechanical behavior of the dry sliding contact between pads and brake rotors using ANSYS. Both full and ventilated rotors were analyzed. The thermal distribution obtained was used to position the ventilation system properly. They demonstrated the role of ventilation system in cooling the discs. They demonstrated that there is definitely a difference in the maximum temperatures reached in ventilated and solid discs used under the same conditions. Higher temperatures are reached in the solid discs as compared to ventilated. It was also proved that temperature and stress in the braking phase are fully coupled. The highest temperatures are reached at the contact surfaces between the disc and the pads. Uneven and high gradient distribution of temperature at the surfaces of disc and pads result in thermal distortion, called as coning and is the main cause of Disc Thickness Variation (DTV). It is also observed that there is a rise in temperature till maximum temperature followed by fall after certain time of braking.

Sung Pil Jung, Young Guk Kim and Tale Won Park [22] found out the shape optimization of the ventilated disc to minimize the temperature and thermal deformation

using response surface analysis method. The thermal energy calculated from the vehicle speed and mass is applied as a heat flux on the disc surface. The contact temperature is a factor combining the effects of load, speed, coefficient of friction and the thermo-physical properties of the system. The brake discs used in vehicles require rapid cooling to increase their performance to prevent thermal deformation and temperature rise during braking. The ventilated disc is lighter than the solid disc, and additional convective heat transfer takes place due to ventilation system. So the temperature rise can be controlled in a better way in ventilated disc but may result in higher uneven distribution of temperature and faster rise in temperature due to removal of material resulting in lesser thermal capacity. So the thermal capacity and thermal deformation were kept in account while modifying the changes.

Pyung Hwang and Xuan Wu [23] did the investigation of temperature and thermal stresses in ventilated disc brake using 3D thermo-mechanical coupling model. They worked on the single brake analysis to stop the vehicle in which the brakes are applied continuously till the vehicle stops. The disc material used is gray cast iron with the vehicle decelerating from 100kph to 0 in 4.72 s. It is found that maximum contact pressure on the pads occurs on the leading side (side of the pad with disc entering) and decreases gradually to the trailing side (side of the pad with disc leaving). Higher temperature is found on the surfaces than the inner portion of the disc material. Also temperature is lower in the vanes area because of convection heat transfer.

Daanvir Karan Dhir [24] investigates the influence of the geometry of the rotor i.e. airfoil vents and holes in comparison to the single solid rotor on the temperature rise and disc durability. Using the average braking power calculated from the energy of the vehicle and time of braking, braking torque was determined. This torque was applied on the disc surface which resulted in heat generation. The three rotors used were solid, with holes and with aerofoil vents. It was found out the maximum durability is of the solid rotor but it has the maximum weight and maximum temperature rise. The other two rotors resulted

in lower temperature rise due to availability of greater convection area but have lower life span as compared to the solid rotor. Maximum rigidity is observed of the solid rotor with minimum deformations, while minimum rigidity is of the rotor with the airfoil vents resulting in maximum deformations.

Qifei Jian and Yan Shui [25] investigated the transient temperature field of ventilated disc under the conditions of hard braking. Hard braking is a condition in which the speed of the vehicle is reduced to zero within fractions of seconds. Hard braking results in very steep rise in temperature due to very less time of braking resulting in high braking power to be absorbed the disc brake system. The temperature field distribution of the brake disc is not symmetrical, and there is some gradient in radial, circumferential, and axial directions. Also the contact surface temperature is much higher than the interior portion. Experimental analysis was also carried out to compare actuality of the results obtained through numerical simulation. The test of hard braking was also carried out on vehicle test bench to compare the results obtained. The temperature gradient of the contact areas was found to be greater than the non-contact areas.

A.Yevtushenko and E. Ivanyk [26] investigated the heat and thermal distortion the braking systems. In the short braking conditions, the heat generated has no time heat the complete disc, and hence the temperature of the disc surface is considerably higher than the mean volume temperature. The change of the heat flux and hence the braking power is taken into account. It has been found that high disc temperatures are reached during long braking. Rapid cooling of disc surface occurs in momentary braking. The change of the normal contact area due to thermal distortion has been neglected. It is also noted that the micro-geometry of the disc surface also has great influence on the contact between the disc and the pads.

A.A Yevtushenko and P. Grzes [27] studied axisymmetric FEA of temperature in a pad/disc brake system with temperature-dependent coefficients of friction and wear in a

single braking process. Two materials of pad FC-16L(retinax) and FMC-11 (metal ceramic) and one material of disc (cast iron) were analysed. With regards to time of braking, the braking period can be divided into four phases. The duration of the first $0 \leq t < t_1$ is determined from the time of an increase in the load acting on the contacting bodies. According to the experimental data, the time from 0 to t_1 equals about2% of the total braking time t_s. This period is characterized by the high speed of sliding, the high flash temperature occurred on micro contacts, the low temperature of contact surface of friction and low temperature gradients normal to the contact surface. The volumetric temperature does not reveal any changes. During the second period $t_1 \leq t < t_2$ the speed remains high, the load reaches nominal value, the flash temperature passes through a maximum point, the temperature and its gradient on the contact surface are high, and the volumetric temperature increases. In the interval of time $t_2 \leq t < t_3$ the speed is still quite high, the load is constant, the flash temperature decreases, the surface temperature reaches maximum value, and the temperature gradient begins to decreases the volumetric temperature increases. In the last, fourth period of braking ($t_3 \leq t < ts$) the speed is close to zero, the load is constant, the flash temperature practically equals zero, the temperature on the contact surface smoothly decreases and brings nearer the volumetric temperature, and the temperature gradient is very small. Duration of this period ranges from3% to 5% from general time of braking.

2.3 RESEARCH GAPS

The extensive review of literature carried out for the present study reveals that numerical thermal analysis has been done previously for the disc brake by

1st method- In one of the methods, the total kinetic energy possessed by the vehicle is calculated based on the total mass and velocity. Then heat flux is calculated using the kinetic energy, and then applied on the specific portion of disc surface in the simulation. In this method, the heat flux is applied on the entire disc ring rather than on the pad-disc actual contact region. This method is used to obtain the temperature distributions, temperature gradients, thermal stresses, etc.

2nd method- In another method, frictional torque is provided to the disc as an external load which results in heat generation. The frictional torque is calculated as the average value considering the braking power and angular velocity. By this way heat generation takes place in the disc and pad, and results of heat flux, temperature distribution, maximum temperature reached are calculated.

Both the above methods which are used to simulate the temperature distribution, maximum temperature, temperature gradients, etc. have some limitations in bringing the actual contact conditions between the disc and the pad. They lack in presenting the actual conditions occurring between the pad and disc. To overcome this, a more genuine method is presented in the present work.

2.4 MOTIVATION

From the above research gaps it can be concluded that though a lot of research has been done in thermal analysis of the disc brake, but the methods used in numerical analysis have some limitations. The present work tries to bring the actual condition in the simulation in with appreciable degree of accuracy.

As discussed above, the first method will not give the exact distribution of temperature on the disc and pad surface since there is a deviation from the actual conditions as heat flux is applied on the disc ring rather than the contact region.

The second method also has its limitation in the sense that contact pressure location between pad and disc varies during braking, so there is not any best value of radius to apply the braking torque.

But the analysis in the current report has been done by bringing the total energy in the disc brake system and then dissipating this energy through real contact between the pads and disc. The total energy possessed by the vehicle during start of braking is brought as the rotational energy possessed by the rotor with some design modifications without changing the disc design and properties. As we know that we are only making the brake system where we require the complete energy possessed by the vehicle to be converted

into thermal energy. So the total energy possessed by the vehicle needs to be provided in some manner to the disc along with the hub part. In the analysis done, density of hub portion material has been increased by around 255 times and it is attached to the disc. Now the rotational energy possessed by the disc and hub part is equivalent to the total energy possessed by the vehicle mass. This kinetic energy is dissipated as heat by the frictional contacts with the pads. This method is more matching the actual conditions and will give better distribution of temperatures and values. Due to the real contact between the pads and disc, kinetic energy will be dissipated as frictional heat. This frictional heat will increase the temperature of the disc and pads.

2.5 OBJECTIVES

In the present work, actual contact condition between the disc and pad has been used in the simulation to obtain temperature distribution. The aim is to dissipate the kinetic energy through real contact between the disc and pads. This contact will result in friction and generation of thermal energy which would give better thermal results. This is done by developing the model of the disc brake using ABAQUS 6.14 with some design changes, choosing of the rotor materials depending on their properties, performing numerical simulation based on the properties obtained for the front disc brake using energy conservation method, and comparing with analytical results.

Furthermore, on the basis of the literature survey the following objectives are identified:

1. Selection of a suitable material for a brake disc on the basis of thermo-mechanical properties and ease of manufacture out of the possible candidate materials viz. ALMMC, DCI, GCI and MSS.
2. Modeling and simulation of an actual brake disc along with a friction pad for a predetermined braking torque capacity of a motor bike.
3. Determination of maximum temperature rise during braking using an analytical model based on single stop braking condition.
4. Comparison of results obtained by simulations with that of the results obtained from analytical model.

CHAPTER 3

RESEARCH METHODOLGY

The research methodology adopted is discussed in detail as below. The entire research is carried out in different stages: developing the model of the disc brake using ABAQUS 6.14 with some design changes, choosing of the rotor materials depending on their properties and use as disc, performing numerical simulation based on the properties obtained for the front disc brake using energy conservation method, and comparing with analytical results.

The numerical analysis has been performed in the following steps:

1- The CAD model has been developed in the ABAQUS CAE comprising of two pads, solid support, modified hub portion, back-plates and disc with the same shape and size as of the actual front disc of Apache RTR 160 which is shown in Fig. 3.1 and 3.2.

2- To minimize the time for analysis, caliper etc. are not modeled. Pads along with back plates have been used with proper boundary conditions without using caliper.

3- Material properties are defined for the disc, pads, solid support, hub and back-plate portions. The assembly of all the components is made as in the actual case.

4- Frictional interaction is defined between pads and disc. A contact is also established between the back-plates and the pads so that the pads don't move due to the reaction forces from the disc.

5- Thermal boundary condition of initial temperature of $35^{o}C$ has been allotted to two pads, and disc.

6- Rotational energy equivalent to the total kinetic energy of the vehicle is provided to the hub and disc merged part.

7-Meshing has been done with tetrahedral coupled-temperature displacement (C3D4T) elements for both the pads and disc. For solid support, hub, and back-plates 3D stress elements (C3D8R, C3D4R) are used according to the requirements.

Various assumptions have been taken into consideration for the simulation which are listed as below:

1- Radiation cooling is neglected since the time of braking is less in severe braking.
2- The analysis is based on combined thermal and mechanical loading.
3- The analysis is done taking distribution of braking force on the front wheel as 70%.
4- Material of disc brake and pads are homogenous and isotropic.
5- Disc material has constant value of properties for the developed temperature range.
6- Pad material has temperature dependent properties.
7- The kinetic energy is lost through the disc brake system, therefore no heat loss occurs between the tyre and road surface.
8- There is no locking of wheels during braking.
9- The analysis is performed for single stop braking conditions
10- Failure due to mechanical reasons is neglected.

3.1 CALCULATION OF INITIAL KINETIC ENERGY, HEAT FLUX, CONVECTION HEAT TRANSFER COEFFICIENT AND ANALYTICAL TEMPERATURE

For the analysis purpose, initial kinetic energy possessed by the vehicle of mass 200kg is given in the form of rotational energy to the disc and hub merged part as shown in Fig. 3.4. The angular velocity of the disc and hub merged part is kept same as the angular velocity of the wheel. As discussed the equality of total kinetic energy of the vehicle and rotational energy of disc brake system is obtained by increasing the density of the hub portion by around 255 times while keeping the properties of disc unchanged. After calculation of initial kinetic and power, heat flux is calculated using the swept area of the disc to be used in the analytical calculations of temperature. The dimensions and various other parameters used in the analysis are mentioned below:

INITIAL KINETIC ENERGY

Outer diameter of the disc= 270mm

Inner diameter of the disc=130mm

Radius of wheel=R=222.1mm

Initial velocity of the vehicle=V_1=54Kmph (15m/s)

Final velocity of the vehicle=V_2=0

Initial angular velocity of wheel or disc= initial angular velocity of disc = $\omega_1 = \frac{V_1}{R} = \frac{15}{0.221}$ =67.5 rad/s

Final angular velocity of wheel or disc=final angular velocity of disc=ω_2 =0

Stopping time=t_s= 1.6s

Deceleration rate=$\frac{V_1}{1.6}=\frac{15}{1.6}=9.375 m/s^2$

Area of pad=0.0021m^2

Swept area of disc on one side=0.032m^2

Mass of vehicle=140kg

Mass of the vehicle along with one person of 60 kg is=200kg

Total energy of the vehicle from the equation (1.5) = Braking energy=$\frac{KmV_1^2}{2}$

=1.05 ×200×15^2/2=23625J

Taking 95% of the energy possessed by the vehicle to be converted into the thermal energy of disc brake system we get= 0.95×23625 J=22445.75 J

As we have seen earlier due to weight transfer to the front axle during braking, more braking is to be applied on the front brakes to provide better control and stability. Taking

70% of the braking action on the front brake, we get 70% of total energy to be dissipated at the front brakes=.7×22445.75=15710.625J

This 15710.625J of energy goes to the complete front brake system comprising of pads and disc both.

With uniform deceleration,
Total P_f(t=0)= braking power at initial moment= $Kma(V_1 - at)$
$=KmaV_1$=1.05×200×9.375×15=29531.25W

Total P_{fav}= Total average braking power=$\frac{K\ m\ a\ V_1}{2}$=14765.625W

Front brake P_f(t=0)= Initial braking power = 29531.25×.95×.7=19638.28W

Front brake P_{fav}=Average braking power= 9819.14W

Braking power at initial moment to be dissipated by the disc= 19638.28×.95W
= 18656.357W (95% goes to the disc as assumed)

Average braking power to be dissipated by the disc= 9819.14×.95W=9328.18W

Braking power on one side of the disc surface (at t=0)=18656.357/2=9328.17W

Average braking power on one side of the disc surface=9328.17W/2=4664.1W

HEAT FLUX

Heat flux=$\frac{\text{Braking Power}}{\text{Swept area of disc}}$

$q_{(0)}$"=initial heat flux =$\frac{\text{Initial braking power}}{\text{Swept area of disc}}$ =9328.17/0.032=291505.98W/m^2

q_0"= average heat flux=$\frac{\text{Average braking power}}{\text{Swept area of disc}}$ =4664.1/0.032=145753.12W/m^2

CONVECTION HEAT TRANSFER COEFFICIENT

Using the Eq. 1.14, the convection heat transfer coefficient is calculated as follows:

Re= Reynolds number= $\frac{p_a V D_{out}}{\mu_a}$

Where, μ_a=1.77× 10^{-5} kg/m-s

p_a=1.2 kg/m^3

V=15 m/s

D_{out}=0.270m

$$Re=\frac{1.2 \times 15 \times .270}{1.77 \times 10^{-5}}$$

=2.74×10^5 (hence turbulent flow)

Therefore, convection heat transfer coefficient is calculated from

h_R=0.04($\frac{K_a}{D_{out}}$) $Re^{0.8}$

Where, K_a=Thermal conductivity of air

h_R=0.04×($\frac{0.026}{0.27}$)(2.74×10^5)$^{.8}$

=86.6W/m^2-k

ANALYTICAL TEMPERATURE VALUES

In this part analytical temperature is calculated for the MSS material in the temperature profile with highest temperature region.

h_R==86.6W/m^2-k

L=0.0024m

K=18W/m-k

First of all,$\frac{h_R\ L}{K}$ values are calculated to determine the $\lambda_1 L$ value.

$\frac{h_R\ L}{K}$=$\frac{86.6\times0.0024}{18}$=0.011546

From the table of transcendental roots, $\lambda_1 L = 0.11$

a_t=$\frac{K}{pC}$= $\frac{18\times3600}{7800\times560}$ = 0.01483m^2/h

t=0.76s=0.000211h

t_s=1.6s=0.00044 h

$\Theta_0(z,t)= \frac{q''_0}{h_R}[2(\frac{\Theta_i h_R}{q''_0}-1)\sum_{n=1}^{\infty} \frac{\sin(\lambda_n L)}{\lambda_n L+\cos(\lambda_n L)\sin(\lambda_n L)} e^{\wedge}(-a_t\lambda^2{}_n t) \cos(\lambda_n Z)+1]$

$q_{(0)}''=291505.98 W/m^2$

$q_0''=145753.12 W/m^2$

$\Theta_i= T_i-T_a=0$

Z=0.0024m

$$\lambda_1 = \frac{\lambda_1 L}{L} = \frac{0.11}{0.0024} = 45.83$$

As discussed previously that only the n=1 term is sufficient to accurate results, so

$\Theta_0(z,t)= \frac{145753.1}{86.6}[2(-1)\frac{\sin(0.11\times57.3)}{0.11+\cos(0.11\times57.3)\sin(0.11\times57.3)} e^{\wedge}(-0.01483 \times 45.83^2 \times 0.000211) \cos(6.3)+1]$

$\Theta_0(z,t)= \frac{145753.1}{86.6}[2(-1)\frac{\sin(6.3)}{0.11+\cos(6.3)\sin(6.3)} e^{\wedge}(-0.01483 \times 45.83^2 \times 0.000211) \cos(6.3)+1]$

$\Theta_0(z,t)=T_0(z, t)-T_\infty= 21.47$ K

After obtaining the above $\Theta_0(z,t)$ using constant heat flux, varying heat flux equation is applied to obtain the final temperature values.

$\Theta(z,t)= \frac{291506}{145753} \times 21.47 - \frac{291506\times3600}{1.6 \times86.6}[0.000211-2 (\frac{\sin(6.3)}{0.11+\cos(6.3)\sin(6.3)})(\frac{\cos(6.3)}{0.01483\times45.83^2})(1-e^{\wedge}(-0.01483 \times 45.83^2 \times 0.000211)=42.94+44.68K$

$\Theta(z,t)=T(z, t)-T_\infty=87.62K$

$T(z, t)=273+35+87.6K=395.62K=122.6^oC$

3.2 MATERIAL PROPERTIES

Disc brake rotor requires high and reproducible coefficient of friction, imperviousness to environmental conditions, ability to withstand high temperature (thermal stability), high wear resistance, flexibility and conformability to any surface, good thermal conductivity

and heat absorption capacity, high strength and durability to sustain torque loads, high vibration damping capacities to minimize the problem of squeal and judder. Based on these requirements, four materials selected are ALMMC, DCI, GCI, and MSS. The properties of these materials are given below in table. These properties are used in the numerical analysis.

Table 3.1 Properties of rotor material

MATERIAL	Young's Modulus (E) GPa	Thermal Conductivity (K) W/m-k	Specific Heat Capacity (C) J/Kg-K	Poisson's Ratio (μ)	Density (ρ) Kg/m^3	Coefficient of Thermal Expansion (α)-(10^{-5})	Thermal diffusivity λ= K/ ρ C mm^2/s
DUCTILE CAST IRON	160	32	506	0.26	7200	1.1	8.81
GREY CAST IRON	135	48	460	0.27	7200	1.15	14.49
ALUMINIUM METAL MATRIX COMPOSITE	130	145	796	0.25	2900	1.2	62.81
MARTENSI-TIC STAINLESS STEEL	190	18	560	0.29	7800	1.1	4.12
PAD MATERIAL	70	3	1300	0.24	2100	1.2	.732

Thermal diffusivity of the materials is calculated from the formula. ALMMC has the maximum value of the thermal diffusivity, while MSS has the minimum value. The highest value for ALMMC material results in higher heat diffusion rate and faster propagation. The various parameters used in the numerical analysis of the model are given in the table 3.2. Table 3.3 gives the values of coefficient of friction along with its variation with temperature. From the literature survey, it has been found that coefficient

of friction increases with temperature to some values of temperature and then it starts decreasing with further rise of temperature.

Table 3.2 Parameters used in designing

Item	Values
Inner disc diameter(ID)	172mm
Outer disc diameter(OD)	270mm
Disc thickness	4.8mm
Angular velocity	68rad/s
Hydraulic pressure	0.3MPa
Stopping time	1.6s
Retardation rate	$9.375 m/s^2$
Vehicle mass	200Kg
Initial speed	15m/s
Area of disc	$0.032 m^2$

Table 3.3: Variation of coefficient of friction with temperature

Coefficient of friction	Temperature (^oC)
0.24	35
0.25	100
0.26	200
0.24	300

3.3 MODEL GENERATION

In ABAQUS software, we can develop the geometry within the same module or we can import it from some other module or CAD software. Being simple in geometry the entire model is developed in the ABAQUS itself. At first translation of the physical problem of the disc brake into the FEA model has been done. A geometric model has been generated which includes Disc, Hub, Brake pads, Solid support and Back-plates using the tools of ABAQUS CAE 6.14. The sketch of disc, pad, hub and 3D image of merged disc- hub part is shown below with all dimensions in mm:

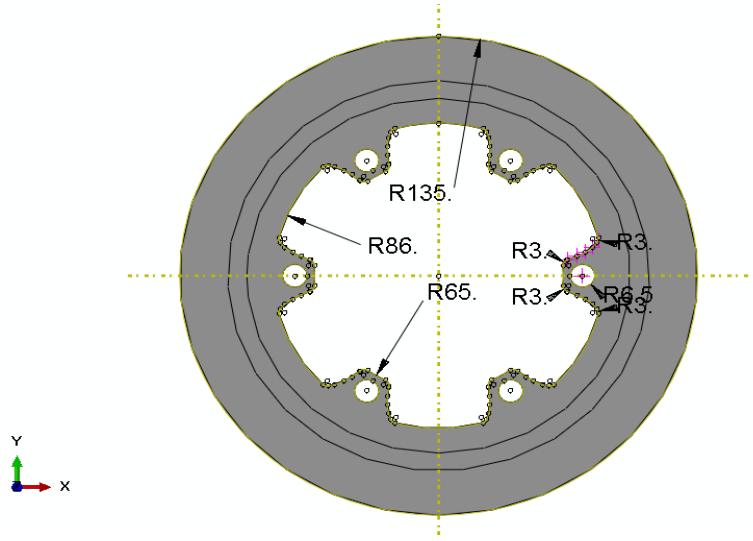

Fig. 3.1 Disc sketch with dimensions

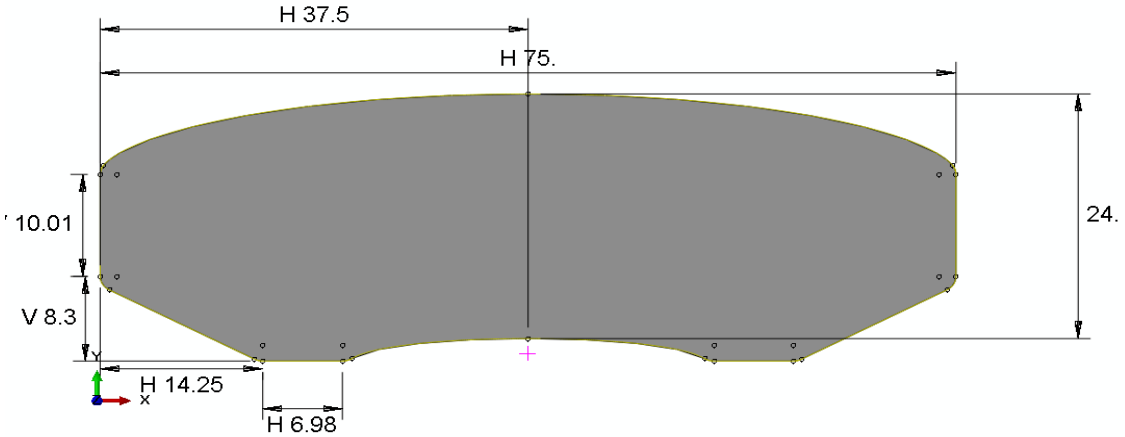

Fig. 3.2 Pad sketch with dimensions

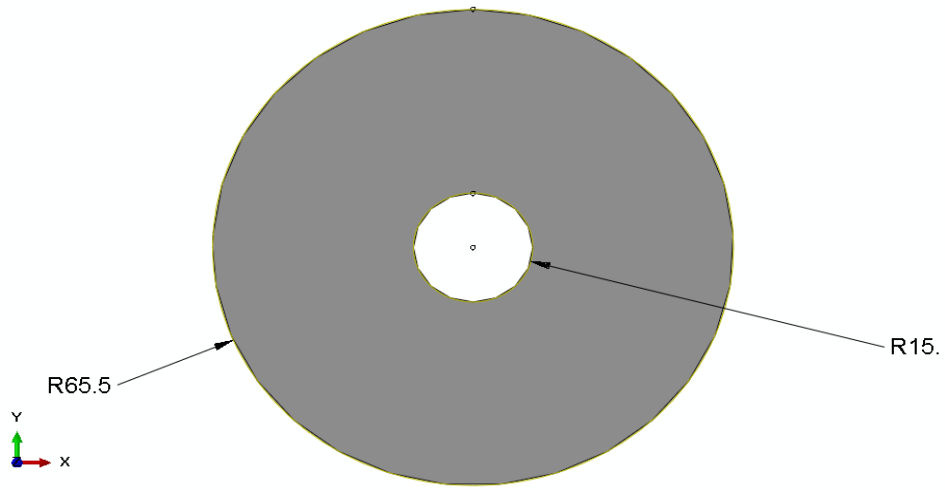

Fig. 3.3 Hub sketch with dimensions

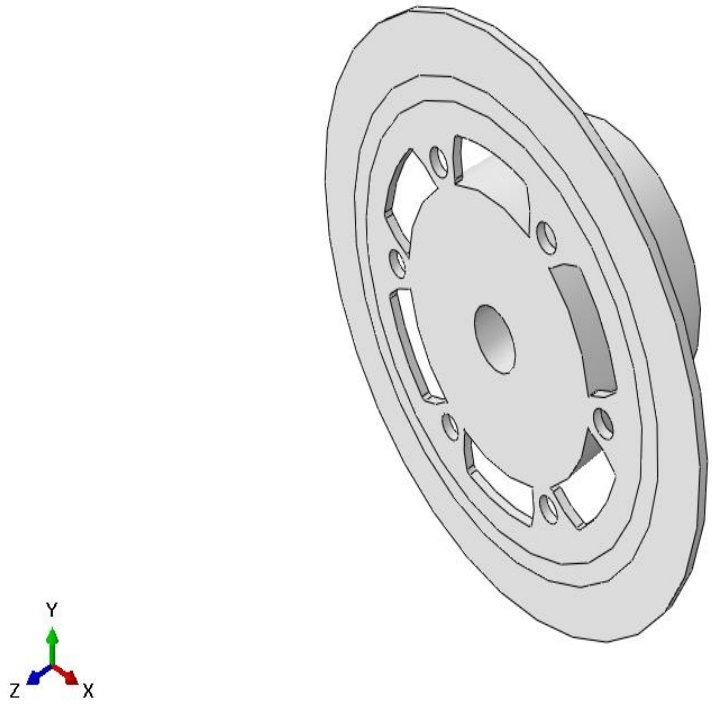

Fig. 3.4 Disc merged with hub

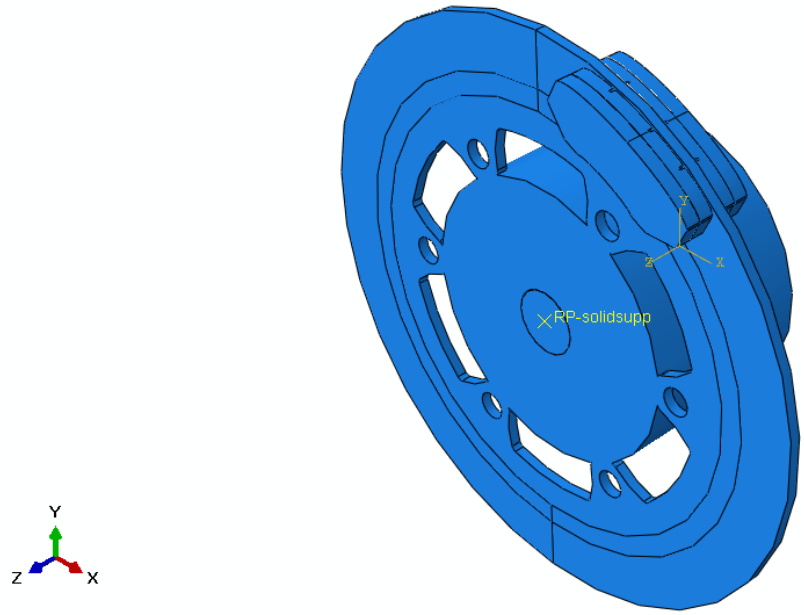

Fig. 3.5 Complete assembly of disc brake system

A geometric model has been generated with components like Disc, Hub, Brake pads, Solid support and back-plates. The shape, size and dimensions of the disc and brake pads are based on the actual dimensions as used in APACHE RTR 160 since temperature distribution need to be analyzed. All this was done in the PART module of the software.

Properties are assigned to all the parts based on the material data. Both thermal and structural properties are provided to disc and pads. This is done in the MATERIAL module. Some changes are made in the density of the hub portion so that the combined disc-hub portion has rotational energy equivalent to that of the total kinetic energy possessed by the complete vehicle. To do so, the density of the hub has been increased by about 255 times as compared to the actual property value.

An assembly is developed with the above parts using global coordinate system. The various parts are positioned with the help of tools available in the ASSEMBLY module. Proper positioning is very important for getting accurate results.

In the STEP module, a dynamic temperature displacement step is created with the total step time of 1.6s. Total 2 steps are there including the initial step. In the initial step, all the boundary conditions required, predefined field and few interactions are defined. In the step-1 i.e. the dynamic temperature displacement step, pressure load and convection heat

transfer is included in addition to the propagated boundary conditions, predefined field, and interactions.

In the INTERACTION module, mechanical and thermal interaction is defined including normal contact, frictional tangential contact, and thermal heat generation between the pads and the disc. Between the solid support and the disc, frictionless interaction is defined so that there is approximately no loss of energy in elastic-plastic deformation of the disc.

In the initial step, predefined field of Initial temperature is assigned to the disc surface and the pads along with other mentioned conditions in the LOAD module.

The last step is of meshing the model as required. For the disc and the pad, coupled temperature displacement elements are used. For other parts, normal 3D stress elements are used. The contact region between the disc and pad is meshed very finely. In the region away from disc pad contact, meshing is kept somewhat coarse so as to reduce the computation time without affecting the efficiency of the results. C3D4T tetrahedral elements are used on both the disc and pads. C3D4tetrahedral elements are used for hub parts and C3D8R elements are used for the back-plates which are not involved in thermal interactions. The table below gives the number of elements, nodes and family for various parts.

Table 3.4 Mesh details of various parts

Serial No.	PAD	DISC	BACKPLATE	HUB
1. Element Type	C3D4T	C3D4T	C3D8R	C3D4
2.No of Elements	8249	18130	3888	143143
3. No. of Nodes	2010	32106	5180	32106
4. Element shape	Tetrahedral	Tetrahedral	Hexahedral	Tetrahedral
5.Geometric order	Linear	Linear	Linear	Linear

CHAPTER 4

RESULTS AND DISCUSSION

The analysis of disc brake is carried out by taking into consideration the different material properties of the ALMMC, DCI, GCI and MSS. The simulation results as well as the analytical results obtained are discussed in the present chapter. There is a discussion on the temperature rise during braking, temperature variation curves, maximum temperature reached and temperature gradients for the different materials. The Fig. 4.1 shows the variation of rotational kinetic energy possessed by the merged disc-hub part in milli Joules with respect to time in seconds. The initial kinetic energy applied in rotational form is same for all the materials in the numerical analysis. Due to friction between the pads and disc surface, the kinetic energy decreases with time as shown in figure and becomes zero in approximately 1.6 seconds. It can be seen that the during start of the braking, fall in kinetic energy is higher as compared to the later part of braking. This can be attributed to the decrease of coefficient of friction after reaching 150-200 ^{o}C.

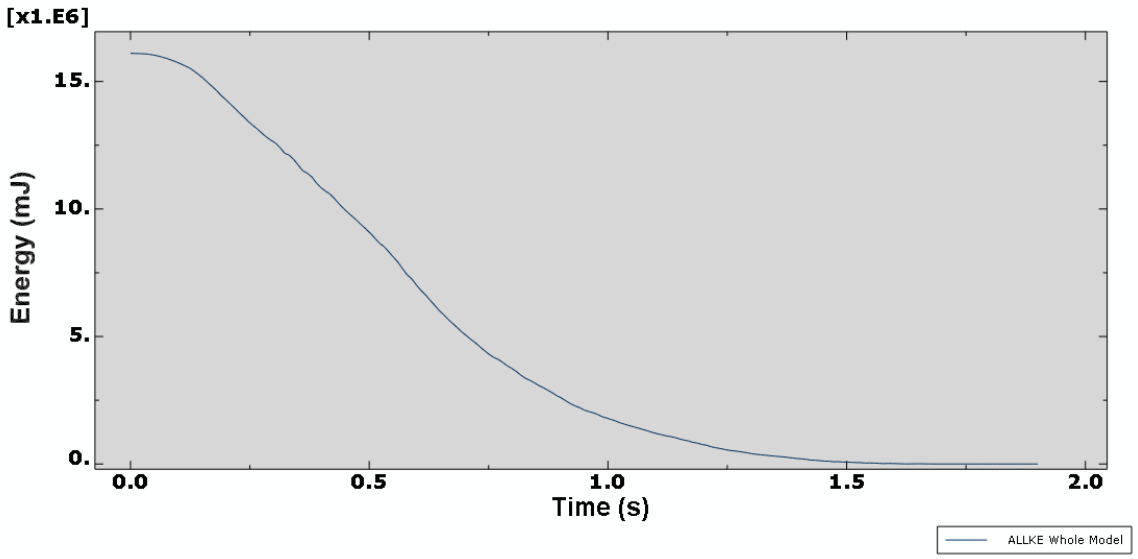

Fig. 4.1 Graph of rotational energy v/s time

The methodolgy used in the numerical analysis is based on the conservation of kinetic energy. The total energy possessed by the vehicle is brought in the rotational form of energy of the combined hub and disc portion. As discussed previously, this is achieved by

increasing the density of the hub portion without any change in the property of the disc. Fig. 4.2 shows the various parts of the assembly of disc brake. In this assembly, the disc is of the same shape, size, and material as is actually used. Changes have been made in the density of the hub part in such a manner that energy equivalence is obtained. Since the braking time is very less, it is assumed that the conduction into the hub part is negligible. The convection heat transfer coefficient is calculated using the equation having a value of 86.6W/m^2-k and is input as the surface film transfer coefficient for the disc and pad surfaces in the simulation.

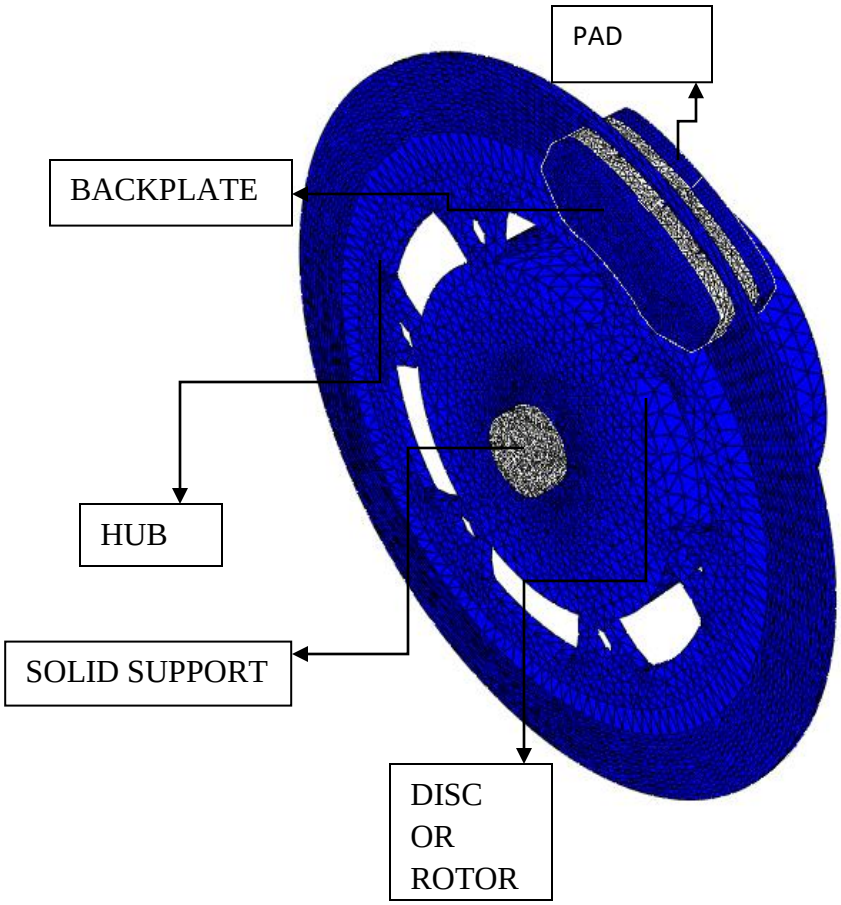

Fig. 4.2 Disc brake assembly with meshing

4.1 TEMPERATURE RISE

The rate of rise of temperature has an important role in magnitude of the thermal stresses developed. Fig. 4.3-4.6 shows the temperature profile of the disc at time 0.4s, 0.6s, 0.8s and 1s for the Aluminium metal matrix composite, Ductile cast iron, Grey cast iron and Martensitic stainless steel respectively. It can be noted that the temperature reaches a maximum value in approximately middle of the total braking time and then decreases for all the materials. The initial strong rise in temperature can be attributed to relatively short braking time in hard braking conditions. Also the initial braking power is higher as compared to the later part as can be noted from Eq. 1.7. We can quickly note that the highest rate of rise of temperature is observed for the Martensitic stainless steel material followed by Grey cast iron. The table 4 below gives the maximum values of temperatures at time 0.4s, 0.6s, 0.8s and 1s for ALMMC, DCI, GCI and MSS.

In all the materials, maximum temperature is observed for the Martensitic stainless steel which is 128.1^{o}C which can be attributed to the minimum thermal diffusivity resulting in higher storage as compared to conduction. In case ALMMC, due to highest thermal diffusivity, the maximum temperature is lowest of all the materials. GCI and DCI show almost similar type of variations.

Table 4.1 Maximum temperature values at different instants of time

Materials	Time (seconds)			
	0.4s	0.6s	0.8s	1s
ALMMC	67.93 ^{o}C	87.18 ^{o}C	83.96 ^{o}C	88.62 ^{o}C
DCI	65.76 ^{o}C	81 ^{o}C	96.4 ^{o}C	92.19 ^{o}C
GCI	68.48 ^{o}C	96 ^{o}C	96.35 ^{o}C	106.8 ^{o}C
MSS	70.99 ^{o}C	97.48 ^{o}C	121.5 ^{o}C	106.3 ^{o}C

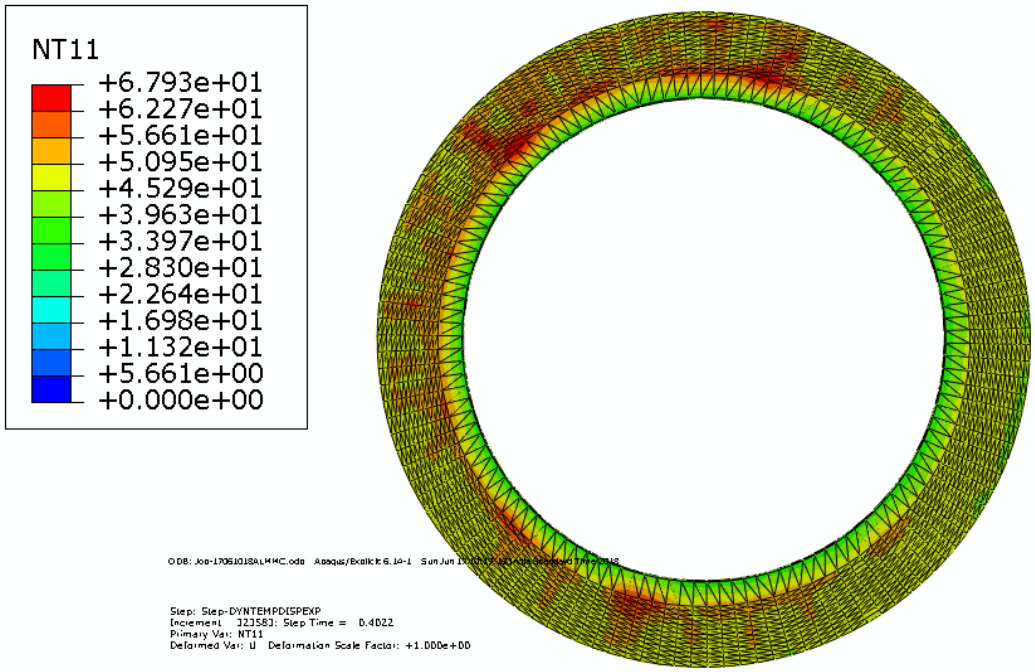

Fig. 4.3.1 Temperature profile of ALMMC after time duration of 0.4s

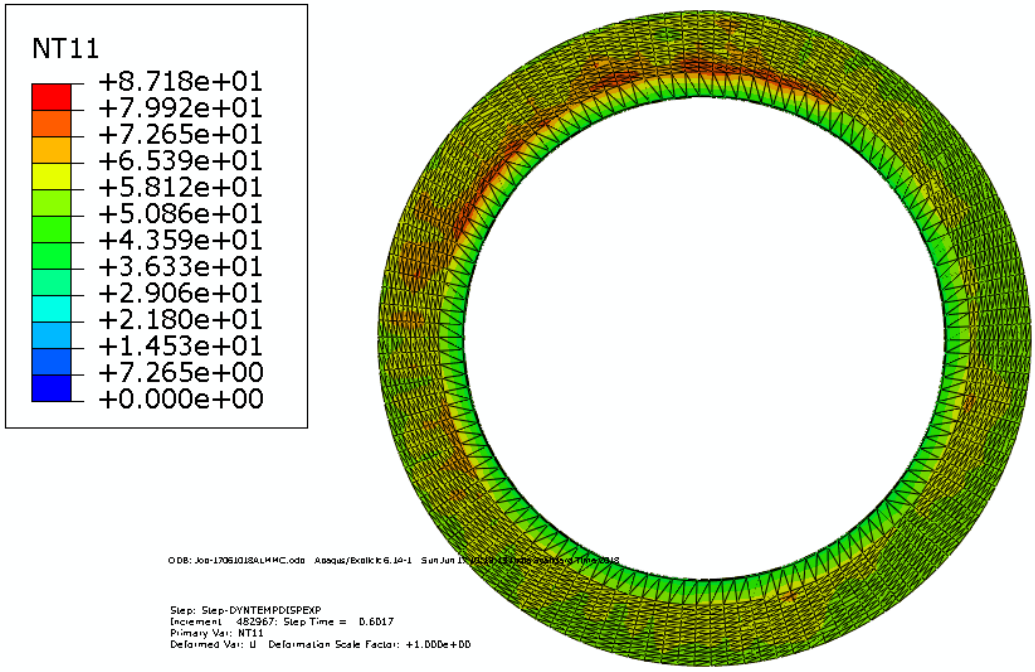

Fig. 4.3.2 Temperature profile of ALMMC after time duration of 0.6s

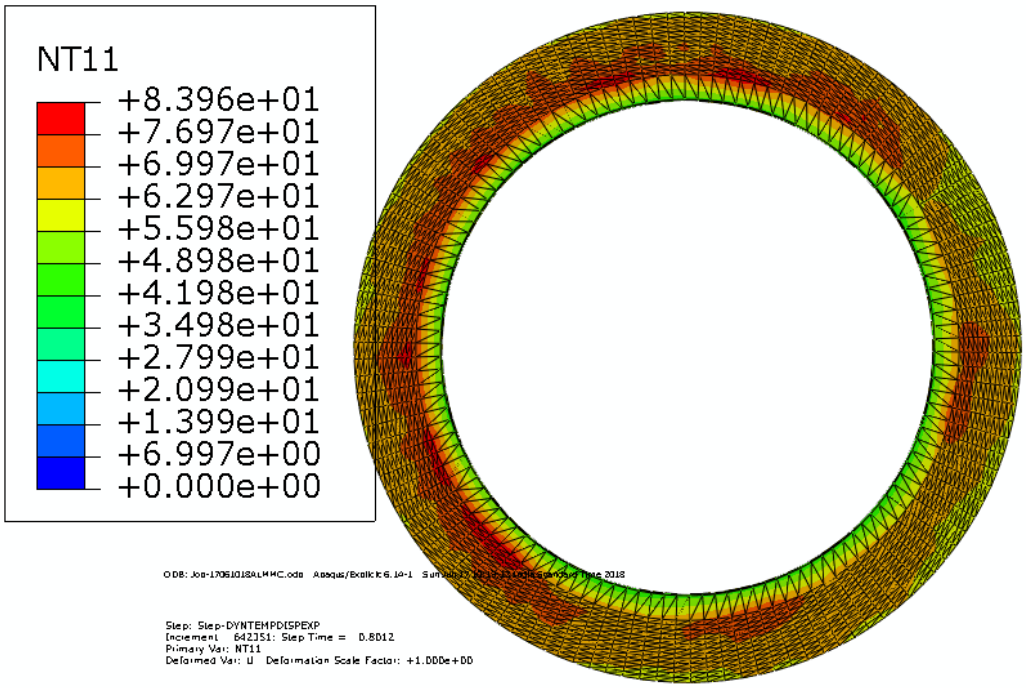

Fig. 4.3.3 Temperature profile of ALMMC after time duration of 0.8s

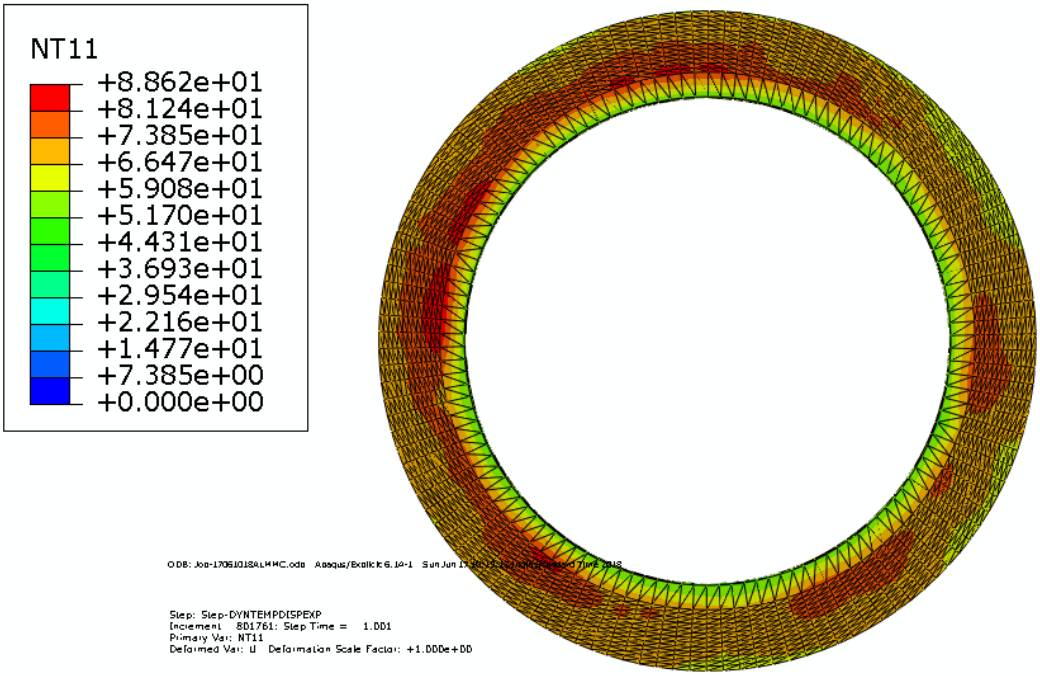

Fig. 4.3.4 Temperature profile of ALMMC after time duration of 1s

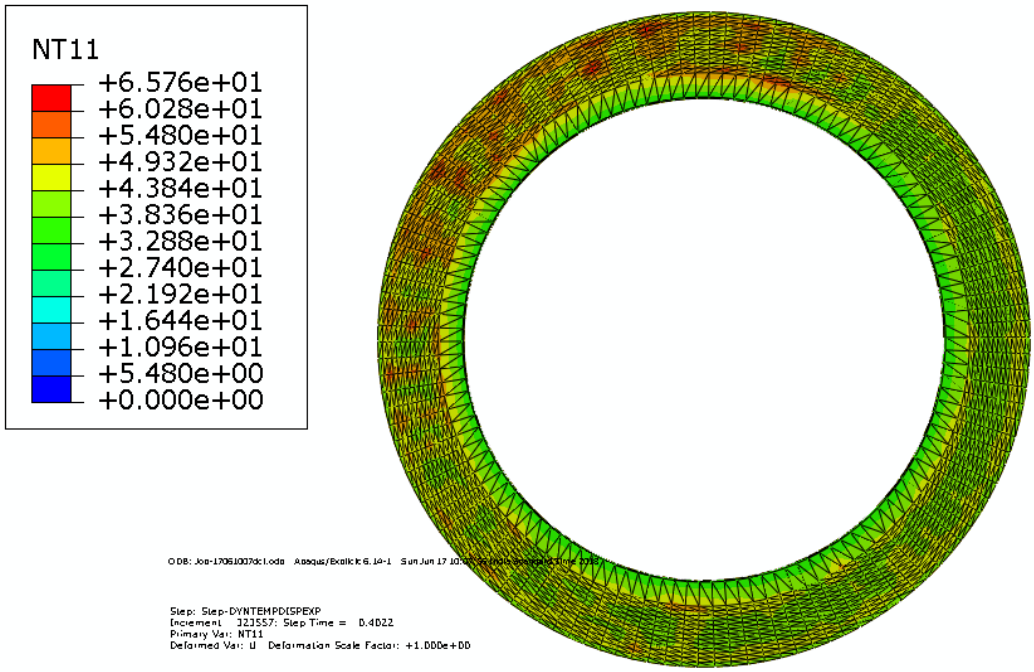

Fig. 4.4.1 Temperature profile of DCI after time duration of 0.4s

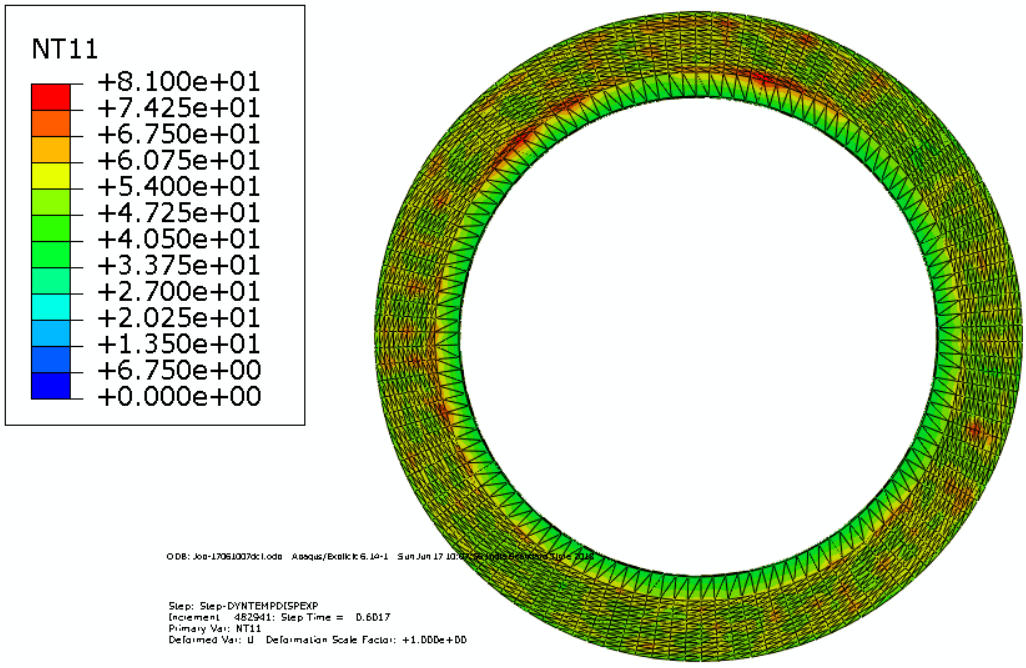

Fig. 4.4.2 Temperature profile of DCI after time duration of 0.6s

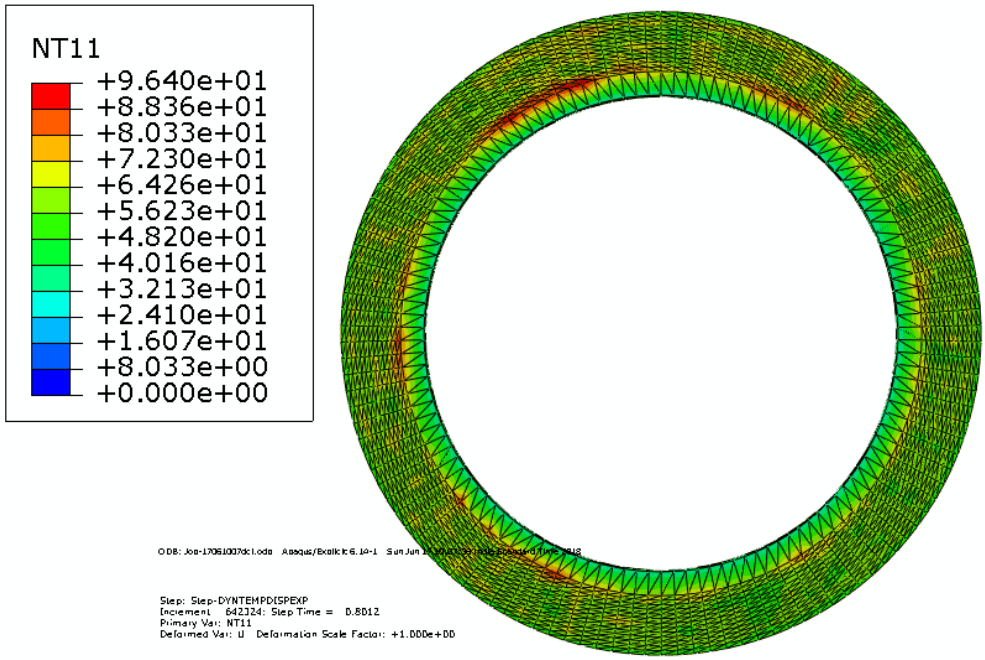

Fig. 4.4.3 Temperature profile of DCI after time duration of 0.8s

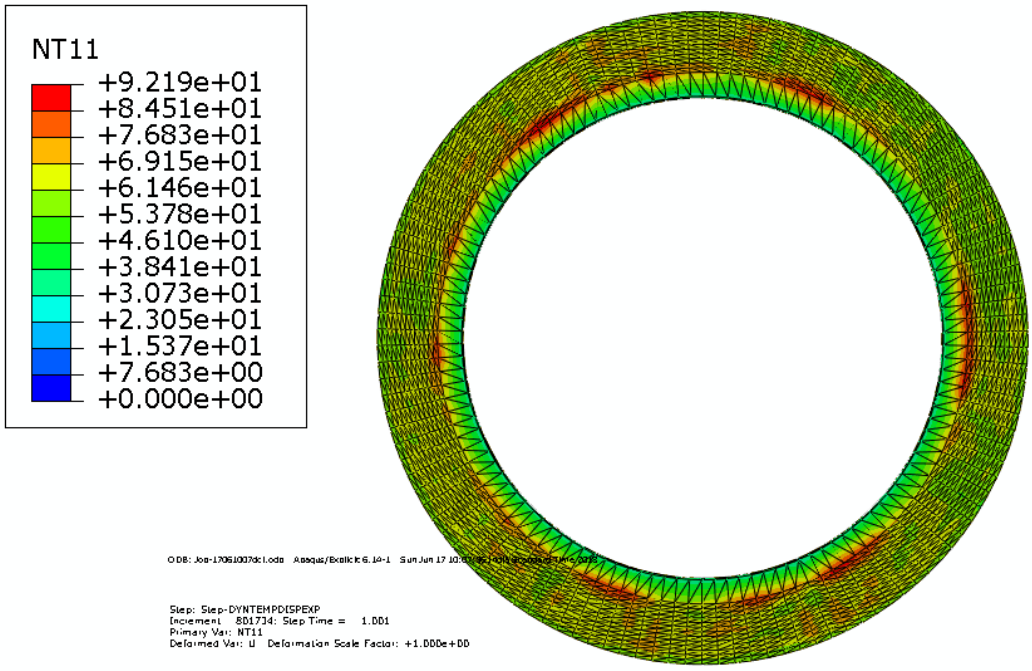

Fig. 4.4.4 Temperature profile of DCI after time duration of 1s

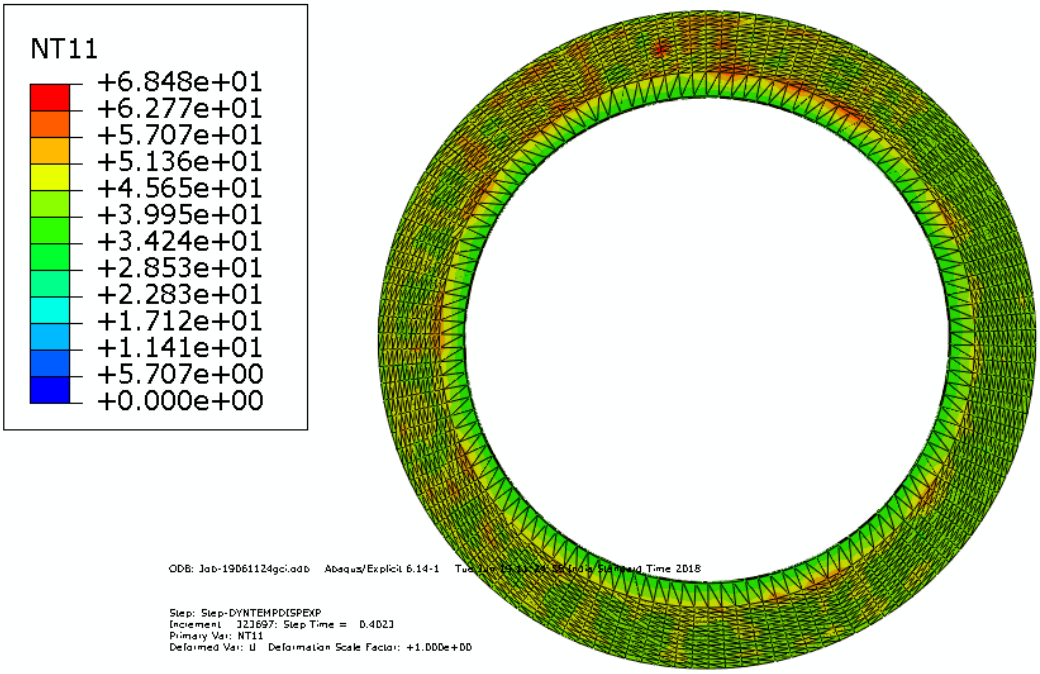

Fig. 4.5.1 Temperature profile of GCI after time duration of 0.4s

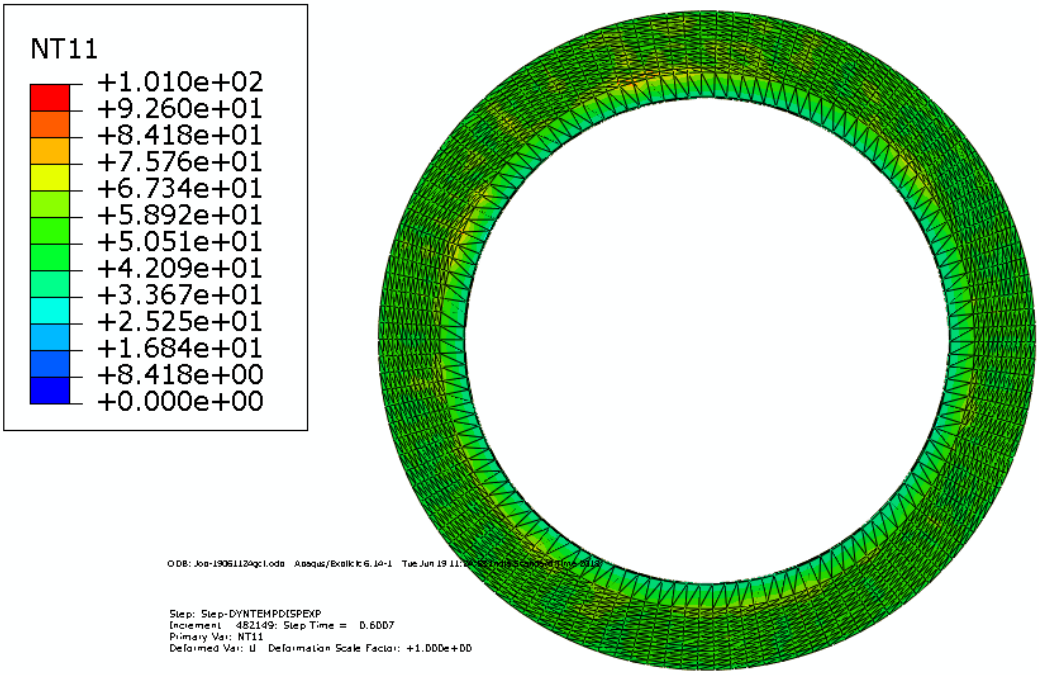

Fig. 4.5.2 Temperature profile of GCI after time duration of 0.6s

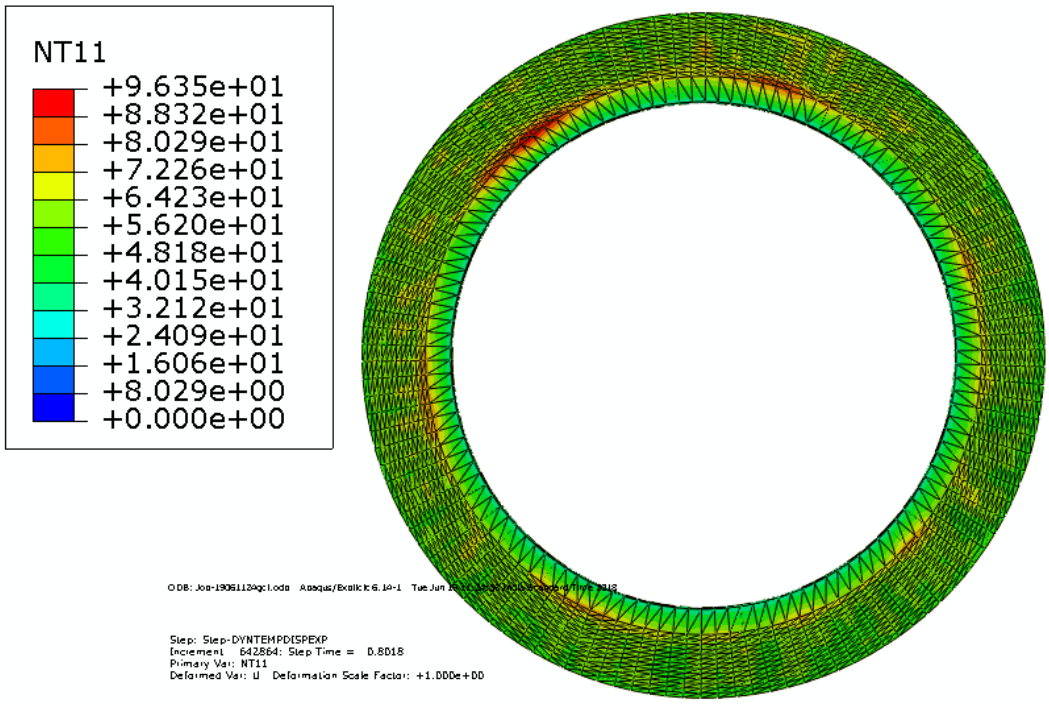

Fig. 4.5.3 Temperature profile of GCI after time duration of 0.8s

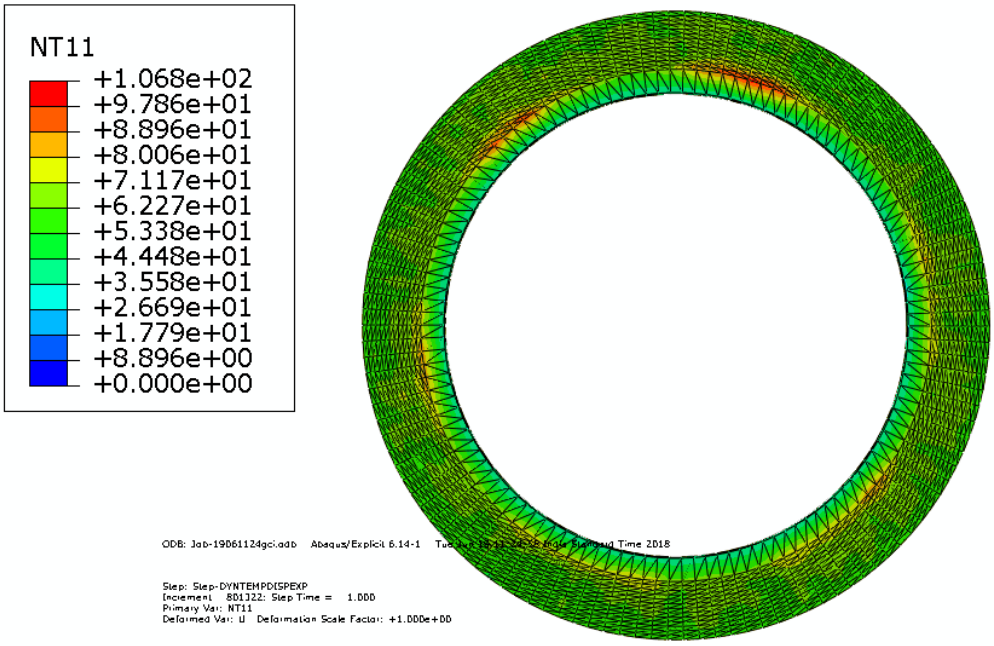

Fig. 4.5.4 Temperature profile of GCI after time duration of 1s

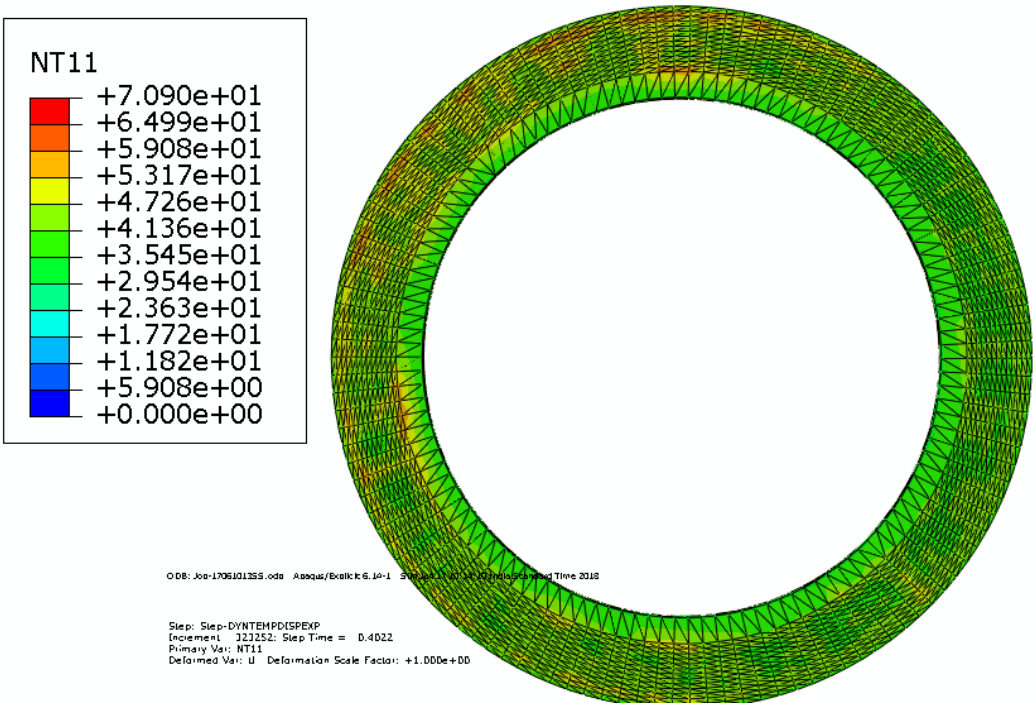

Fig. 4.6.1 Temperature profile of MSS after time duration of 1s

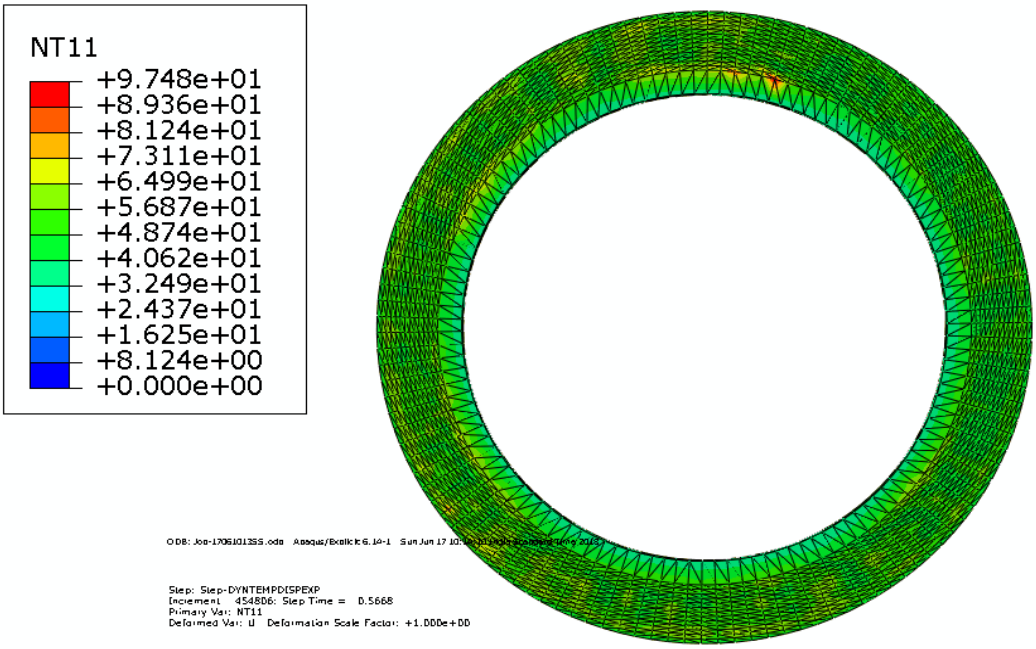

Fig. 4.6.2 Temperature profile of MSS after time duration of 0.6s

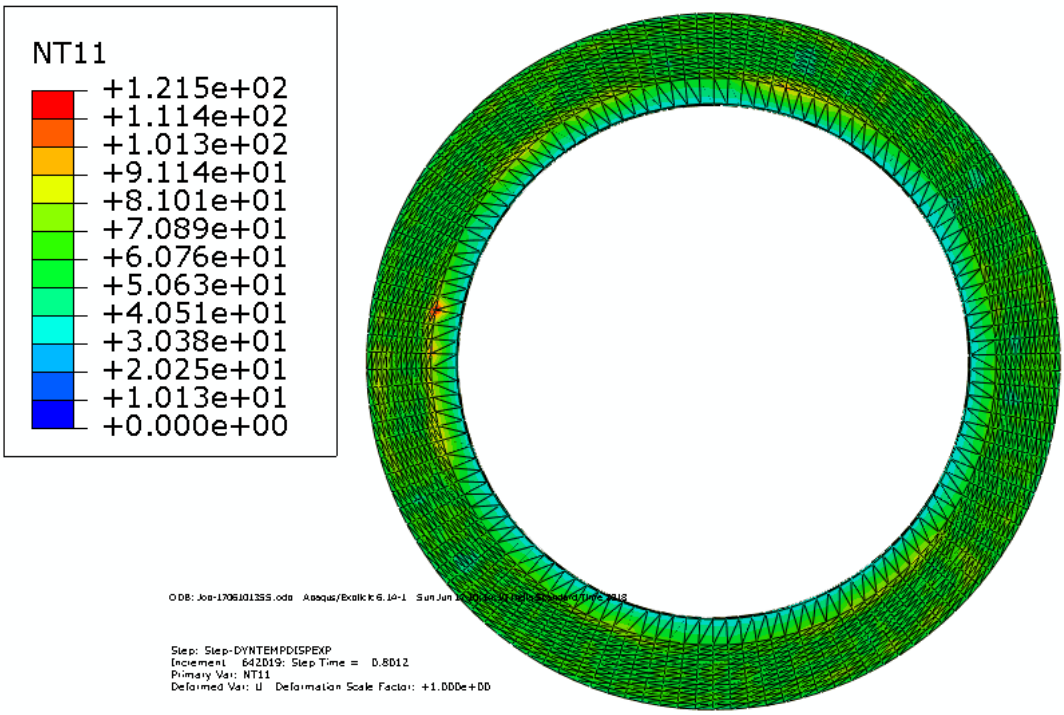

Fig. 4.6.3 Temperature profile of MSS after time duration of 0.8s

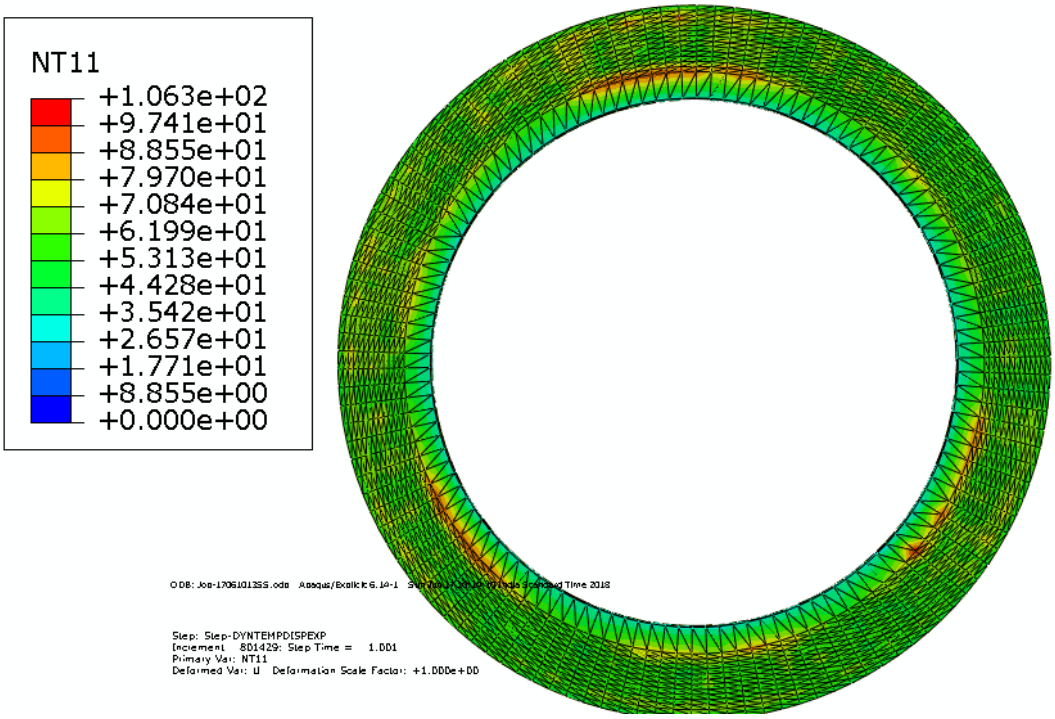

Fig. 4.6.4 Temperature profile of MSS after time duration of 1s

4.2 TEMPERATURE VARIATION CURVES

Friction between the disc and the brake pads results in heat generation. This heat results in temperature rise. Physically temperature of disc surface is measured using rubbing or embedded thermocouples or non-contacting radiation sensors. It has been observed with the help of embedded thermocouples placed in the contact region of the disc and the brake pads, temperature variation is of the form as shown in Fig. 4.7. In the numerical analysis we can see the almost same type of variation at contact region nodes of the disc in the Fig. 4.9.

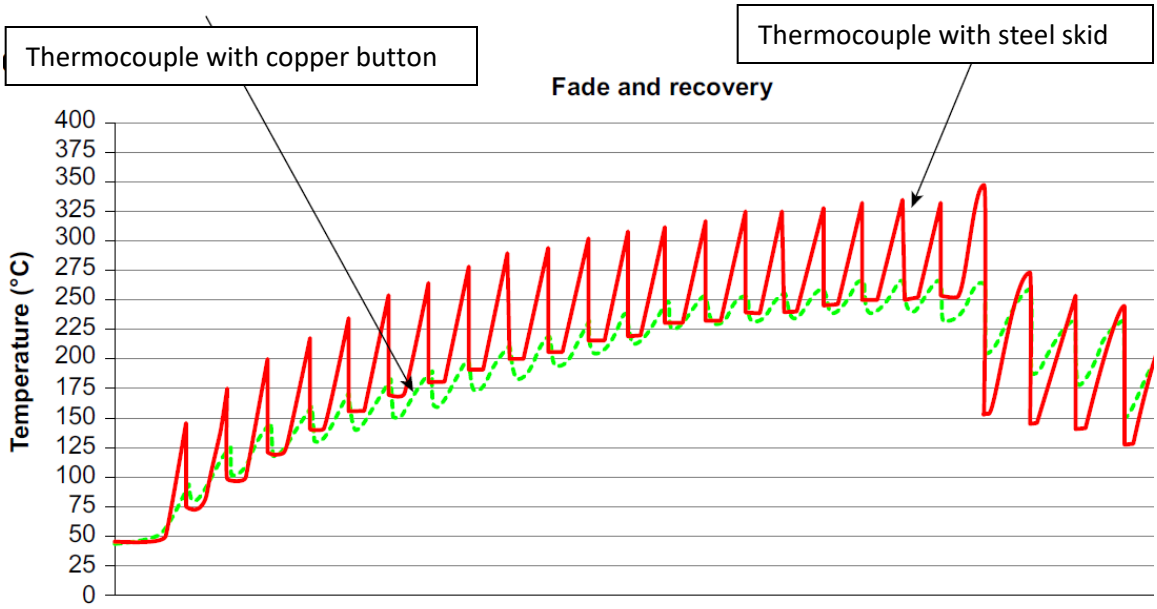

Fig. 4.7 Temperature variation observed at a point of disc using thermocouple [28]

In the present study, total step time of 1.6s is divided into 600 frames using the step module. Hence slight differences can be seen in the curve obtained experimentally and numerically. But the general nature of both the curves is same. The sections 4.2.1, 4.2.2 and 4.2.3 are based on the temperature variations observed at some particular nodes in the maximum temperature condition of the disc. The nodes are selected in the contact region, at outermost radius and at innermost radius.

In section 4.2.1, the node with maximum temperature condition is selected in the contact region and the variation of temperature with respect to time is plotted for 1.6 sec for ALMMC, DCI, GCI and MSS material respectively which can be seen in Fig. 4.9.

In section 4.2.2, the node at the innermost radius in the maximum temperature condition is selected and the variation of temperature with respect to time is plotted for 1.6 sec for ALMMC, DCI, GCI and MSS material respectively which can be seen in Fig. 4.10.

In section 4.2.3, the node at the outermost radius is selected in the maximum temperature condition and the variation of temperature with respect to time is plotted for 1.6 sec for ALMMC, DCI, GCI and MSS material respectively as shown in Fig. 4.11. The nodes selected for the sections 4.2.1, 4.2.2, and 4.2.3 are shown in Fig. 4.8.

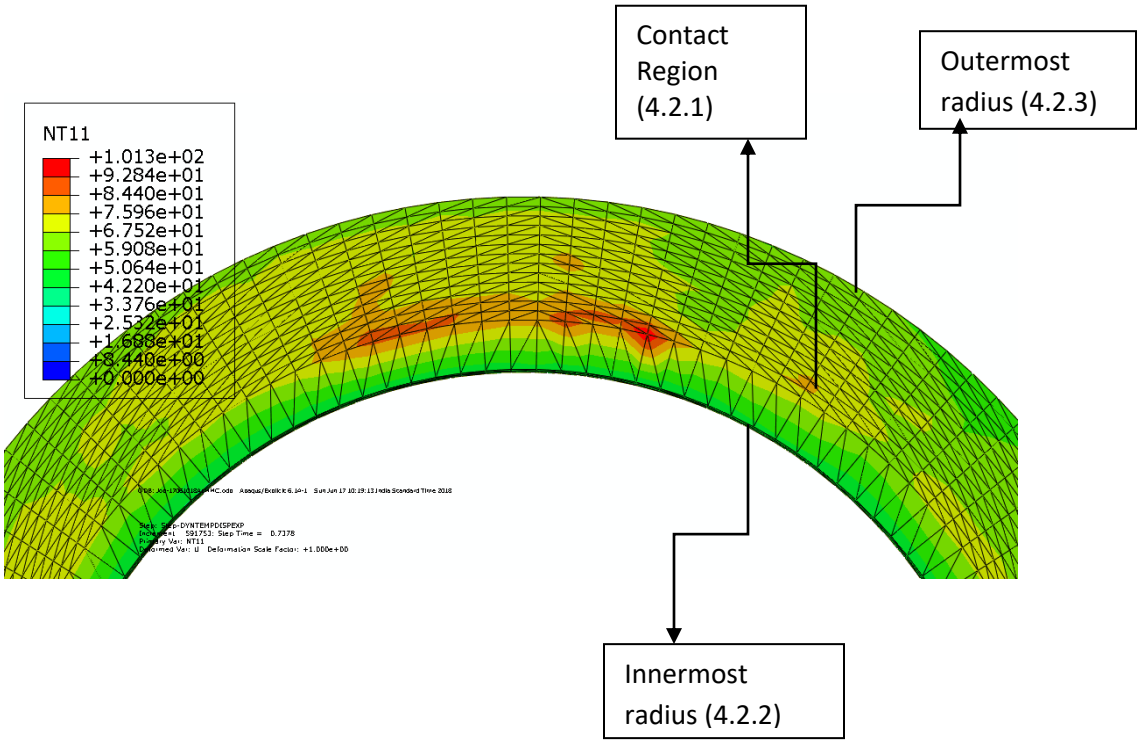

Fig. 4.8 Displaying the nodes selected for saw-tooth temperature curves

4.2.1 SAW-TOOTH TEMPERATURE VARIATION IN CONTACT REGION

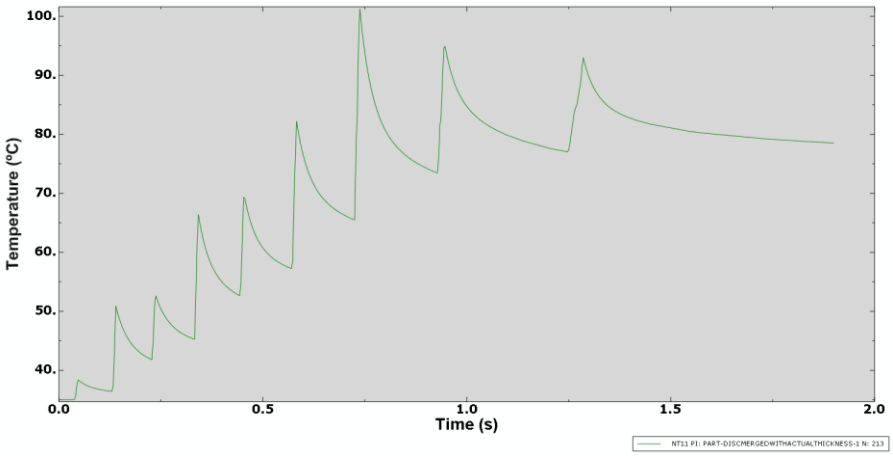

Fig. 4.9.1 Saw-tooth temperature variation for ALMMC in contact region node

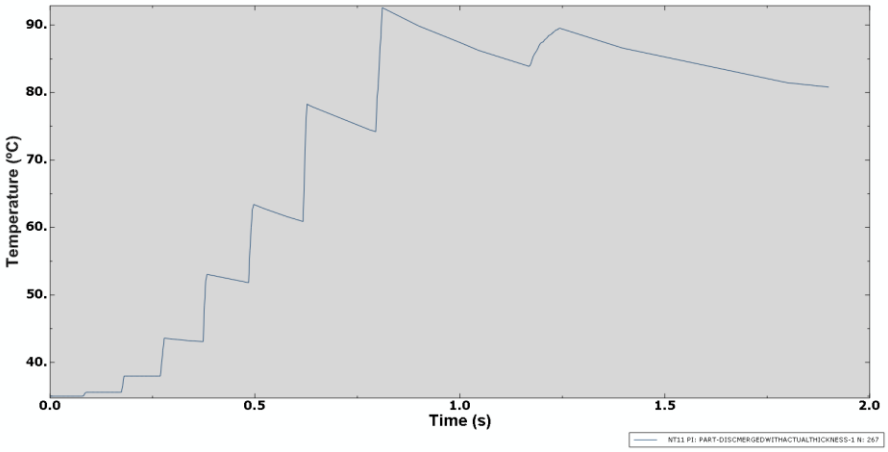

Fig. 4.9.2 Saw-tooth temperature variation for DCI in contact region node

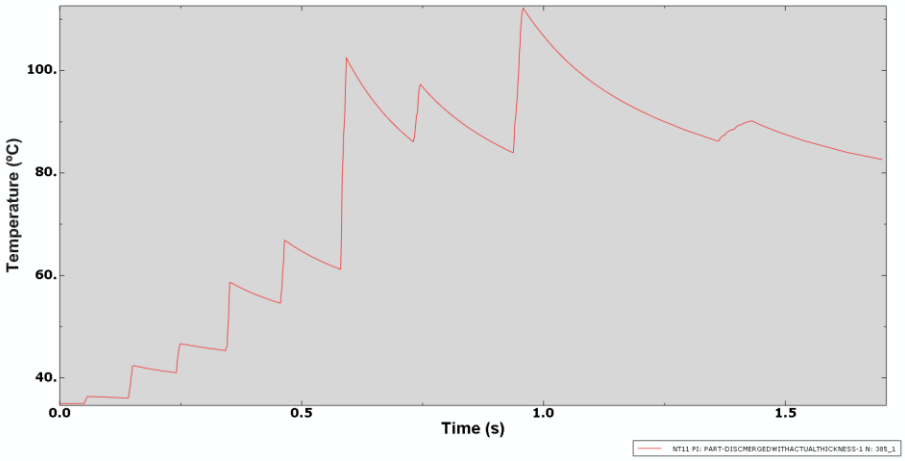

Fig. 4.9.3 Saw-tooth temperature variation for GCI in contact region node

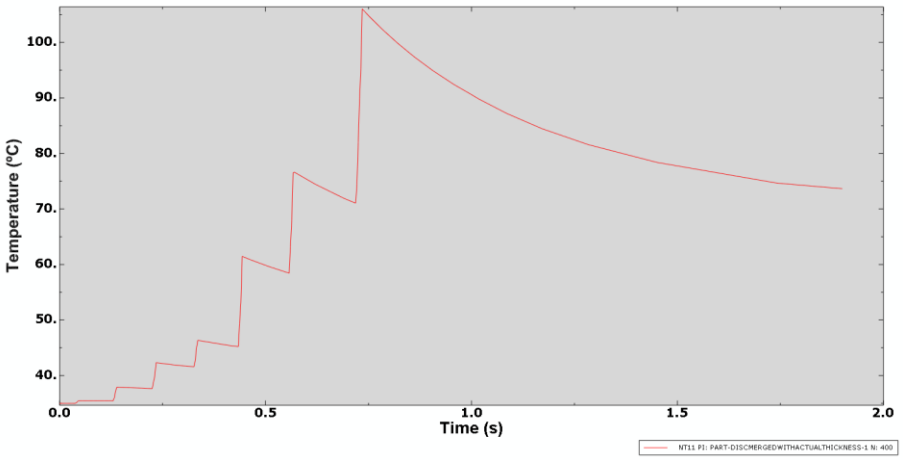

Fig. 4.9.4 Saw-tooth temperature variation for MSS in contact region node

4.2.2 TEMPERATURE VARIATION AT INNERMOST RADIUS

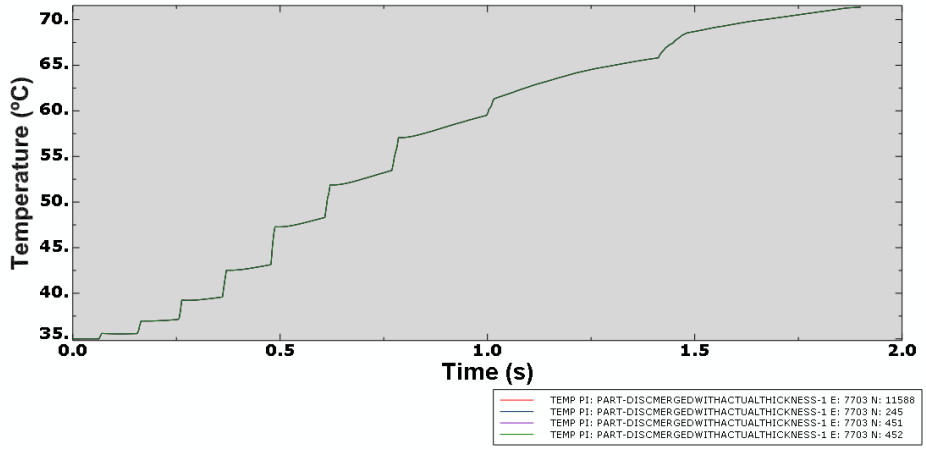

Fig. 4.10.1 Temperature variation for ALMMC at innermost radius node

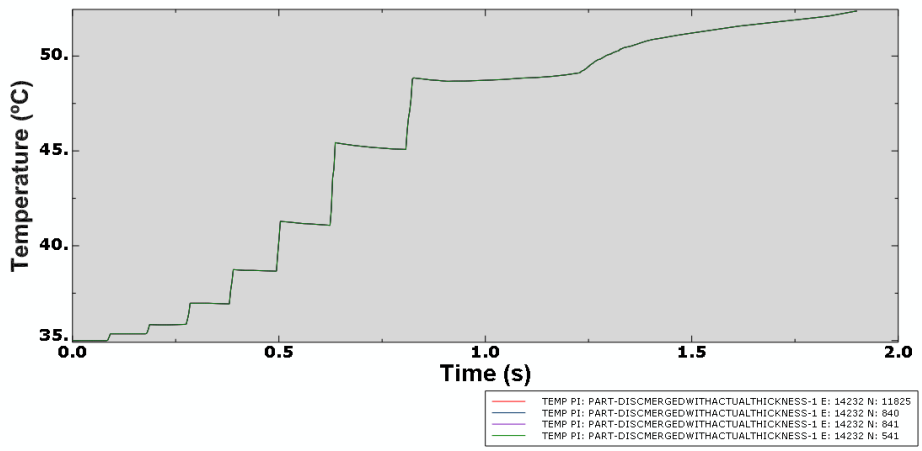

Fig. 4.10.2 Temperature variation for DCI at innermost radius node

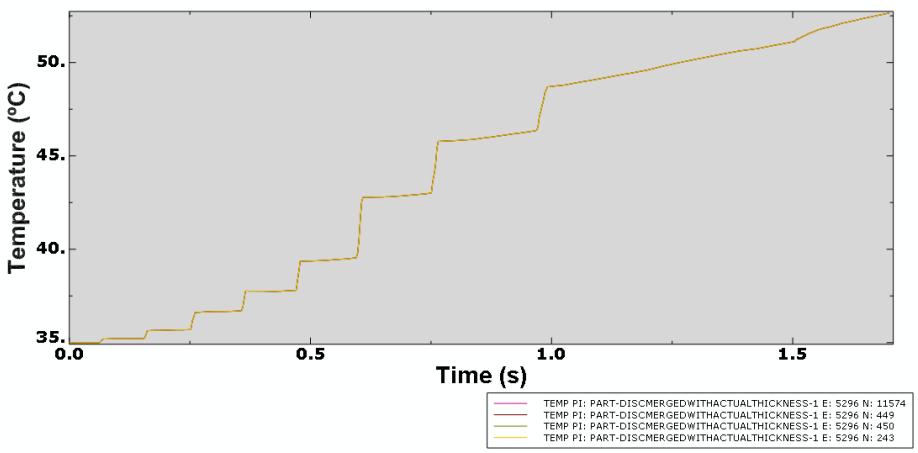

Fig. 4.10.3 Temperature variation for GCI at innermost radius node

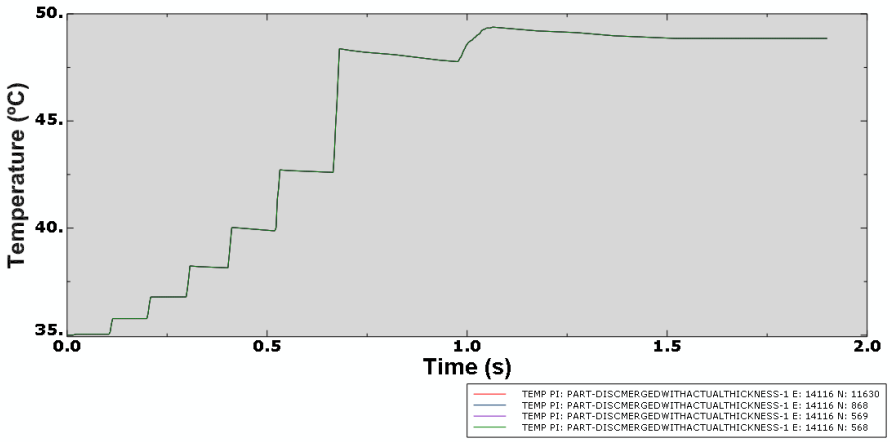

Fig. 4.10.4 Temperature variation for MSS at innermost radius node

4.2.3 TEMPERATURE VARIATION AT OUTERMOST RADIUS

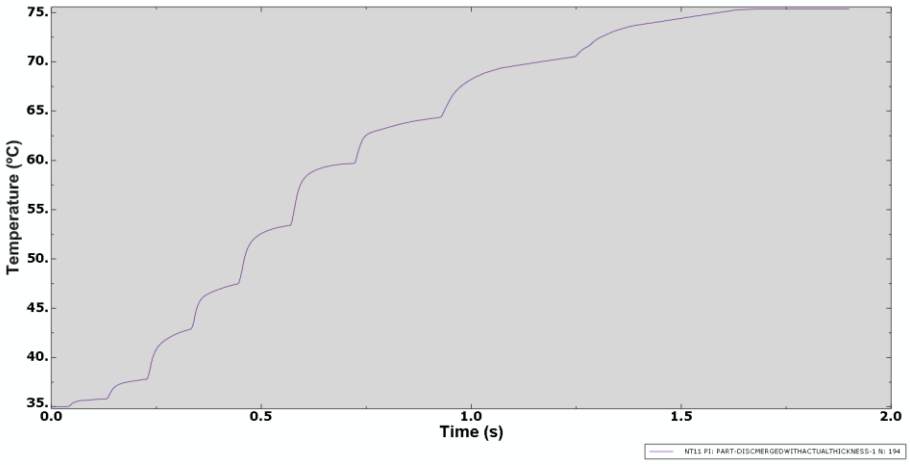

Fig. 4.11.1 Temperature variation for ALMMC at outermost radius node

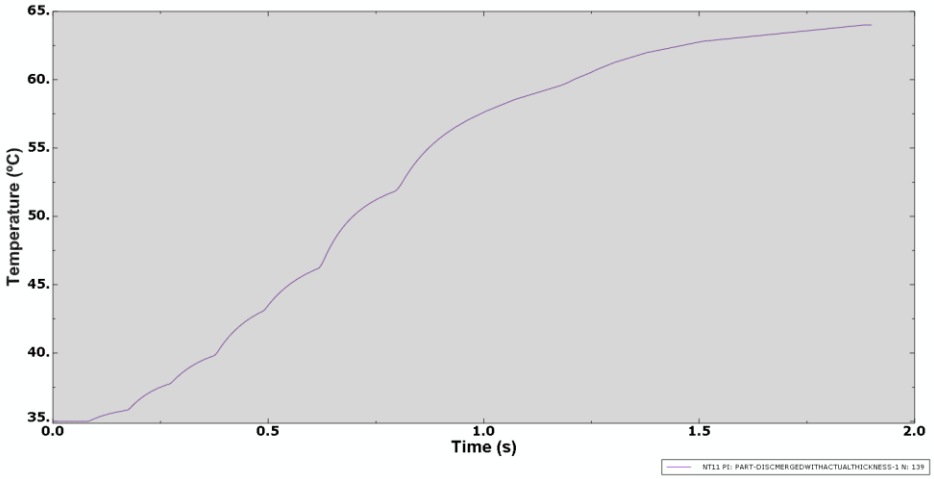

Fig. 4.11.2 Temperature variation for DCI at outermost radius node

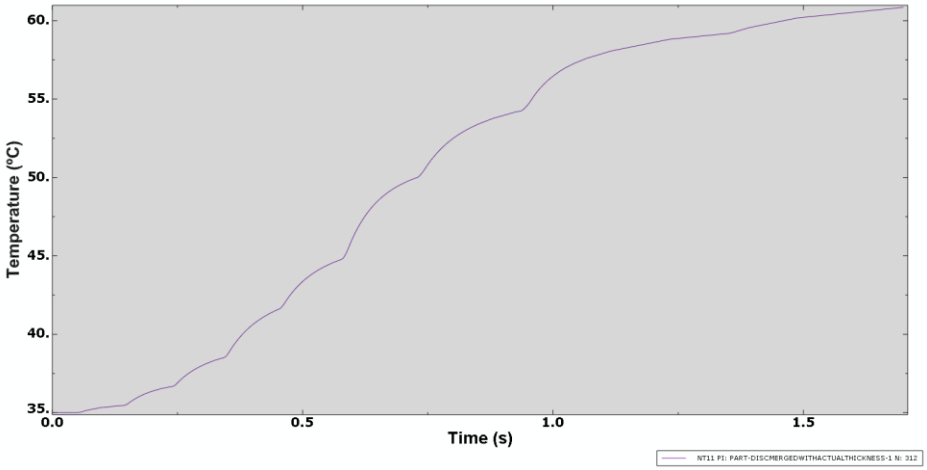

Fig. 4.11.3 Temperature variation for GCI at outermost radius node

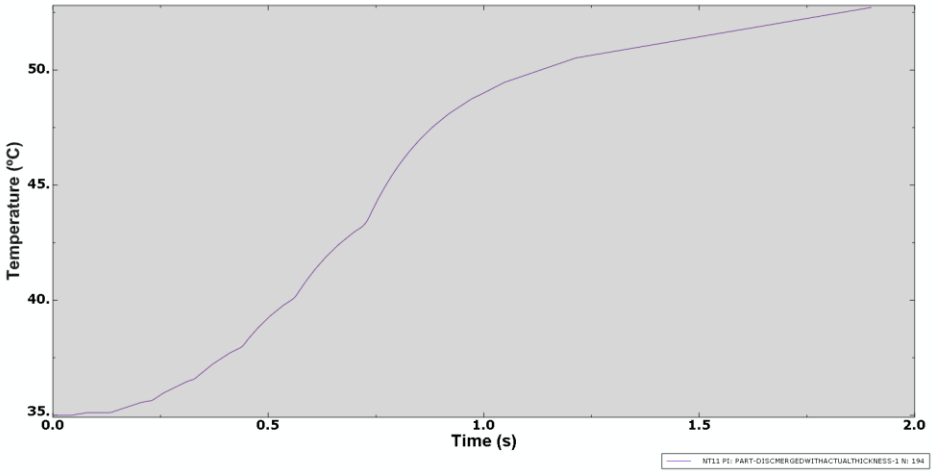

Fig. 4.11.4 Temperature variation for MSS at outermost radius node

The Fig. 4.9-4.11 are in the sequence ALMMC, DCI, GCI and MSS materials for all the sections 4.2.1, 4.2.2, and 4.2.3. As seen from Fig. 4.9, the temperature at the node in the contact region increases as the node passes through the friction contact region between disc and pads which is observed as almost vertical line. Then there is a net decrease of temperature till the node again comes in the frictional contact region after completing one rotation cycle.

In section 4.2.1 with nodes at maximum temperature point, it can be seen that the temperatures rise suddenly to a maximum, and decreases after some time of braking in one rotation cycle. The rise of temperature is observed when the node comes in the frictional contact region after every rotation. Then till that rotation cycle is completed, there is a decrease in temperature. We can see that highest cooling takes place for the contact node in one rotation cycle for ALMMC which is visible by rate of fall. In MSS, the temperature is almost a horizontal type line after the vertical rise initially which means least cooling. This can be attributed to the least thermal diffusivity of the MSS. The reason of this saw-tooth variation is that any particular point on the material gets heated when it enters in frictional contact region. Due to thermal diffusivity, this point will get cooled till the next rotation cycle start.

In section 4.2.2 with nodes at the inner-most radius region, it is seen that the maximum temperature is reached at the innermost radius for the ALMMC material. Due to higher thermal diffusivity of ALMMC, the heat is diffused rapidly to all the regions.

In section 4.2.3 with nodes at the outer-most radius region, least temperatures are observed for the MSS material. This is attributed to the lower thermal diffusivity resulting in more storage of energy then the conduction. For DCI and GCI almost same variation is observed. In case of ALMMC, again due to higher thermal diffusivity, higher temperatures are observed in the outer-most radius region.

4.3 PROFILE WITH HIGHEST TEMPERATURE REGION

In this section, temperature profile is shown for different materials with the highest temperature region. In all the materials, maximum temperature is observed for MSS, followed by GCI, DCI and ALMMC. Also the maximum temperature values are obtained

in approximately the middle of the total braking time which can be seen from the table 4.2. The high initial rise of temperature is due to higher braking power loss in the initial time period as can be seen from the equation 1.7, resulting in maximum temperatures approximately in the middle of the total braking time. Fig. 4.12-4.15 gives the temperature profile in highest temperature region.

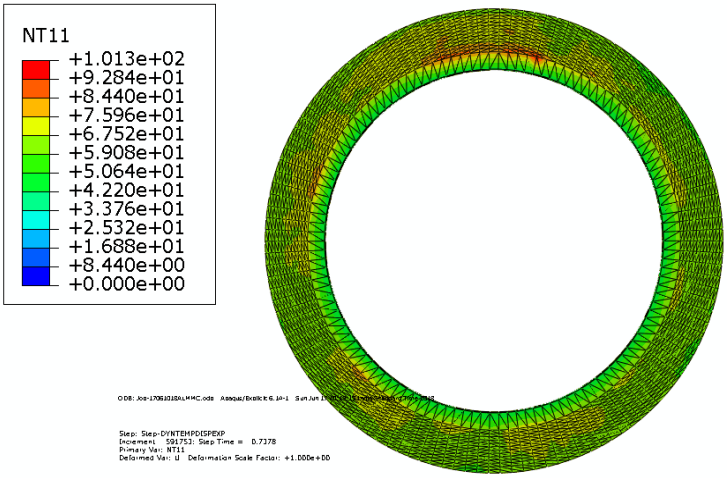

Fig. 4.12 Highest temperature profile for ALMMC

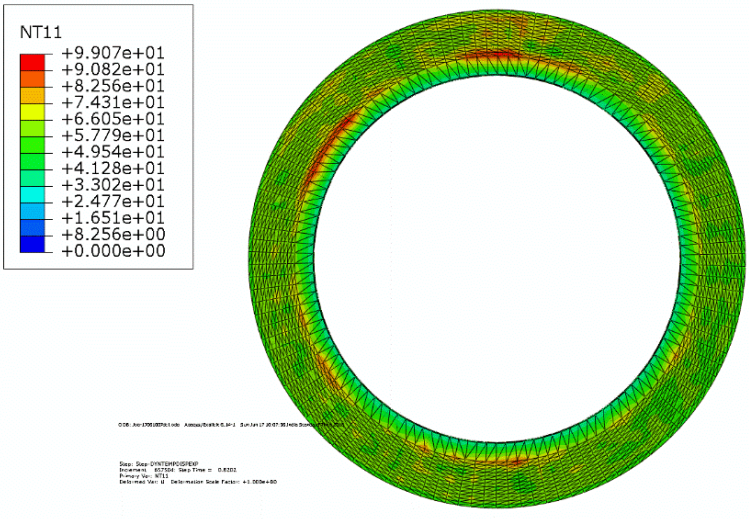

Fig. 4.13 Highest temperature profile for DCI

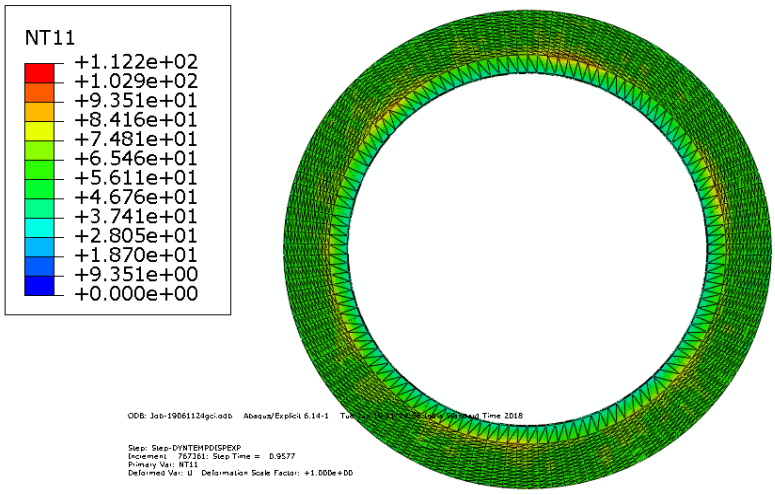

Fig. 4.14 Highest temperature profile for GCI

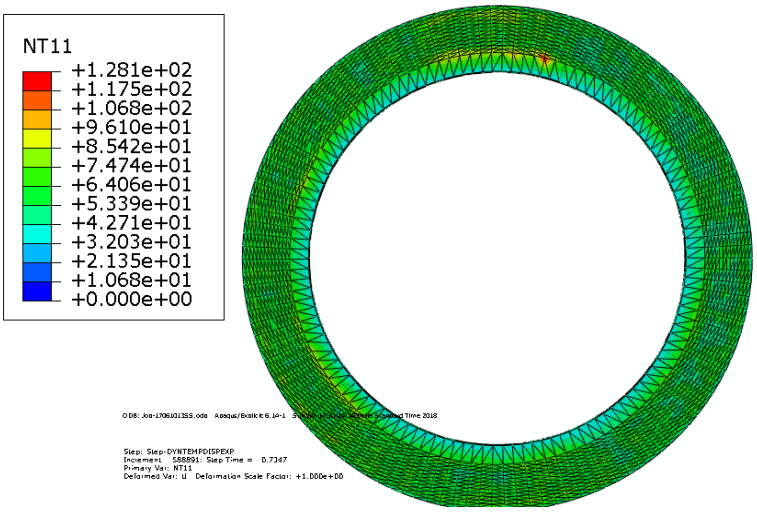

Fig. 4.15 Highest temperature profile for MSS

The table 4.2 gives the maximum temperature (^{o}C) and corresponding time (s) in tabular form.

Table 4.2 Comparison of maximum temperature with time

Disc material	Maximum temperature (^{o}C)	Time (s)
ALMMC	101.3	0.75
DCI	99.1	0.82
GCI	112.2	0.91
MSS	128.1	0.76

4.4 TEMPERATURE GRADIENTS

Temperature gradients are the main reason behind the thermal cracks resulting from high thermal stresses. The section 4.4.1 and 4.4.2 discusses the temperature gradients in the frictional contact regions for ALMMC, DCI, GCI, and MSS after time duration of 0.4s and 1s respectively. These two instants of time are chosen as one depicts start of the temperature rise and other depicts the constancy in temperature values. Temperature gradients can be seen only in the radial and circumferential directions from the 2D figures.

In case of ALMMC in both sections 4.4.1 and 4.4.2 we can see more uniformity of temperature as compared to other materials. This implies heat is more distributed in this case as compared to the other materials. This is due to highest thermal diffusivity of ALMMC as compared to DCI, GCI and MSS materials. In MSS, the temperature is more concentrated in few regions. The higher temperature is in few regions while the rest of the material is at comparatively lower temperatures.

It can also be noted that in all the materials, i.e., ALMMC, DCI, GCI and MSS, temperature gradients are higher near the frictional contact region of brake surface and brake pads as compared to other regions.

4.4.1 TEMPERATURE GRADIENTS IN CONTACT REGION AFTER TIME DURATION OF 0.4s

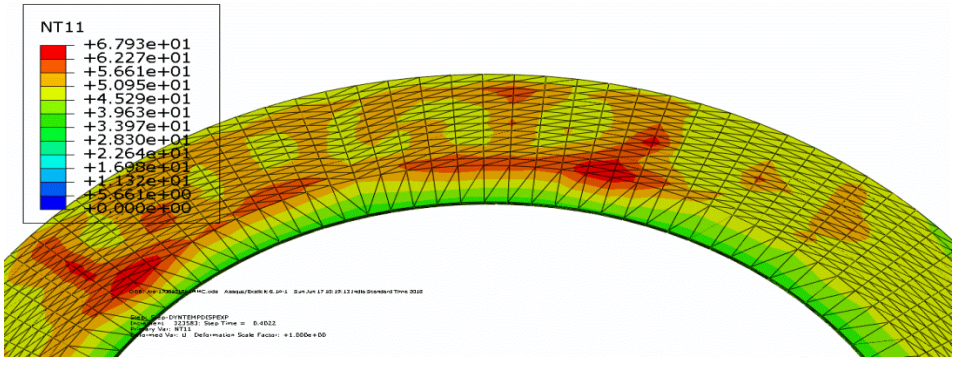

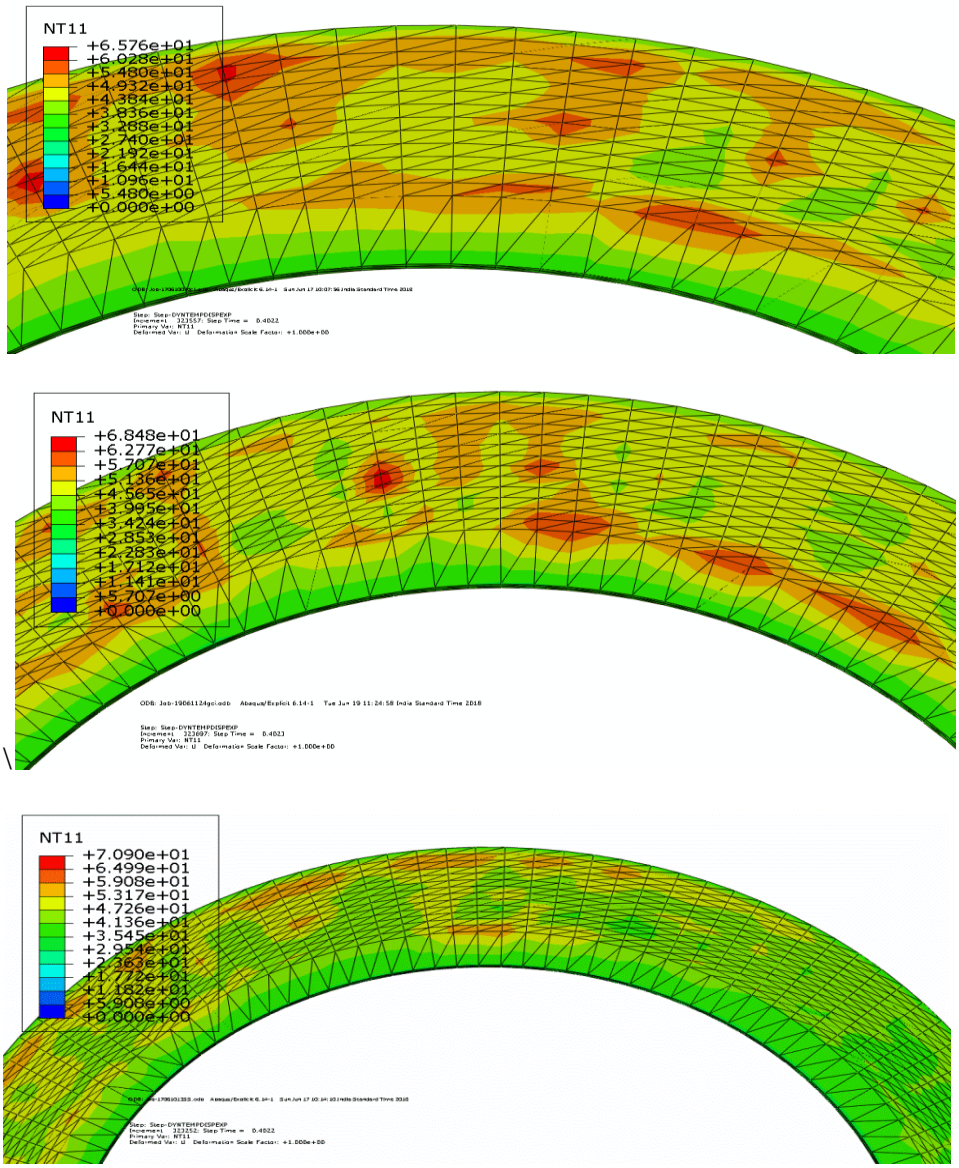

Fig. 4.16 Temperature gradients respectively for ALMMC, DCI, GCI and MSS after time duration of 0.4s in contact region

4.4.2 TEMPERATURE GRADIENTS IN CONTACT REGION AFTER TIME DURATION OF 1s

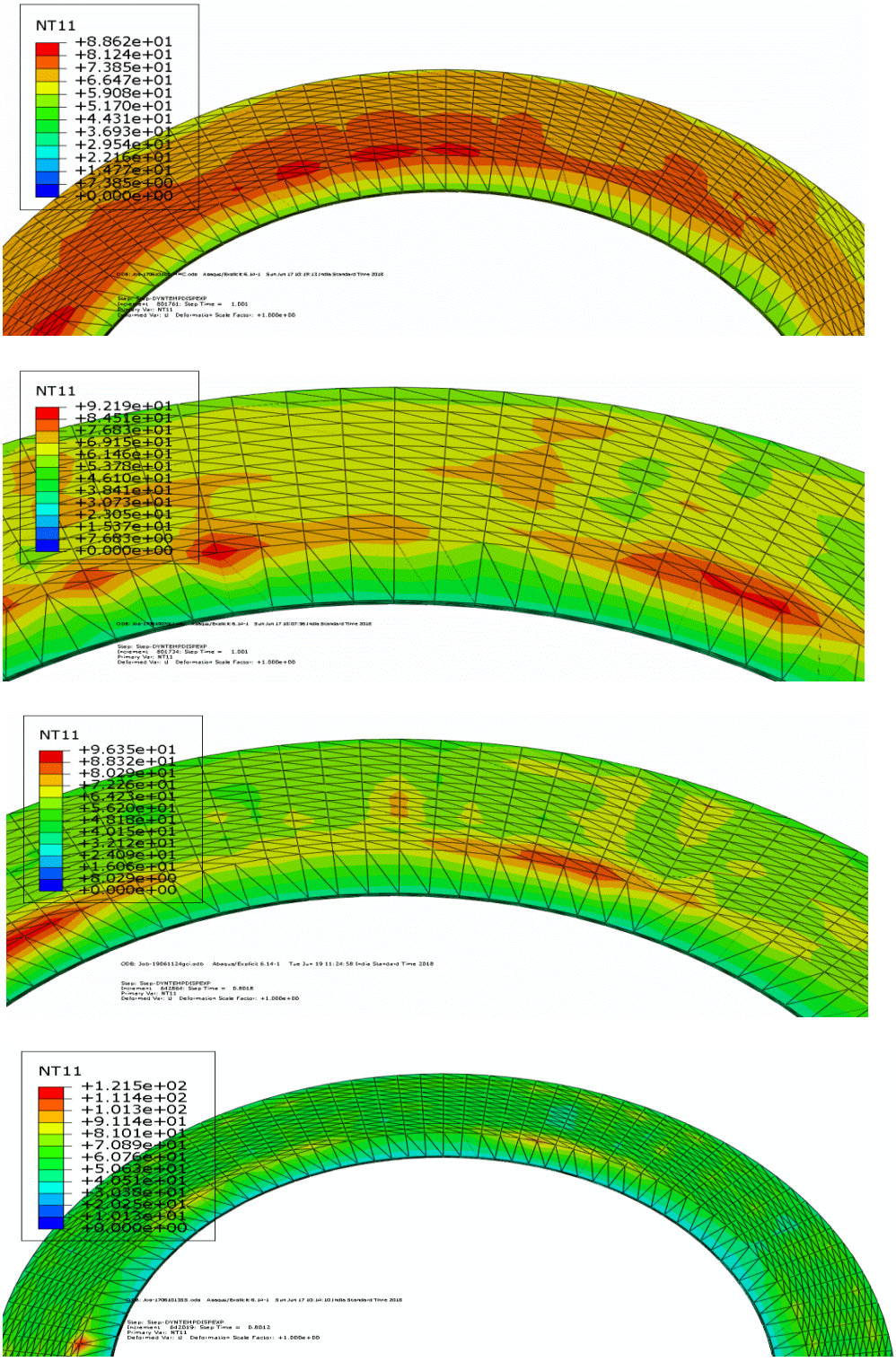

Fig. 4.17 Temperature gradients respectively for ALMMC, DCI, GCI and MSS after time duration of 1s in contact region

4.5 TEMPERATURE DISTRIBUTION IN FRICTION PAD

Friction pads are important considering the thermal stability and wear at higher temperature. These are generally made of lower thermal conductivity as well as lower thermal diffusivity material to prevent brake fluid vaporization. Due to this much higher temperature are there on the surface as compared to the remaining volume of material. These have high value of specific heat capacity. The Fig. 4.18 shows the temperature variations at two different durations of time. From the below Fig. 4.18 it can be concluded that on the contacting surface, higher temperatures are observed at the outer periphery of the pad surface as compared to the central portions of the surface. This may be due to the change in cross-section resulting in higher temperatures. Also due to higher area of contacting region on the bottom side periphery of the pad, higher temperature can be seen as compared to top side periphery.

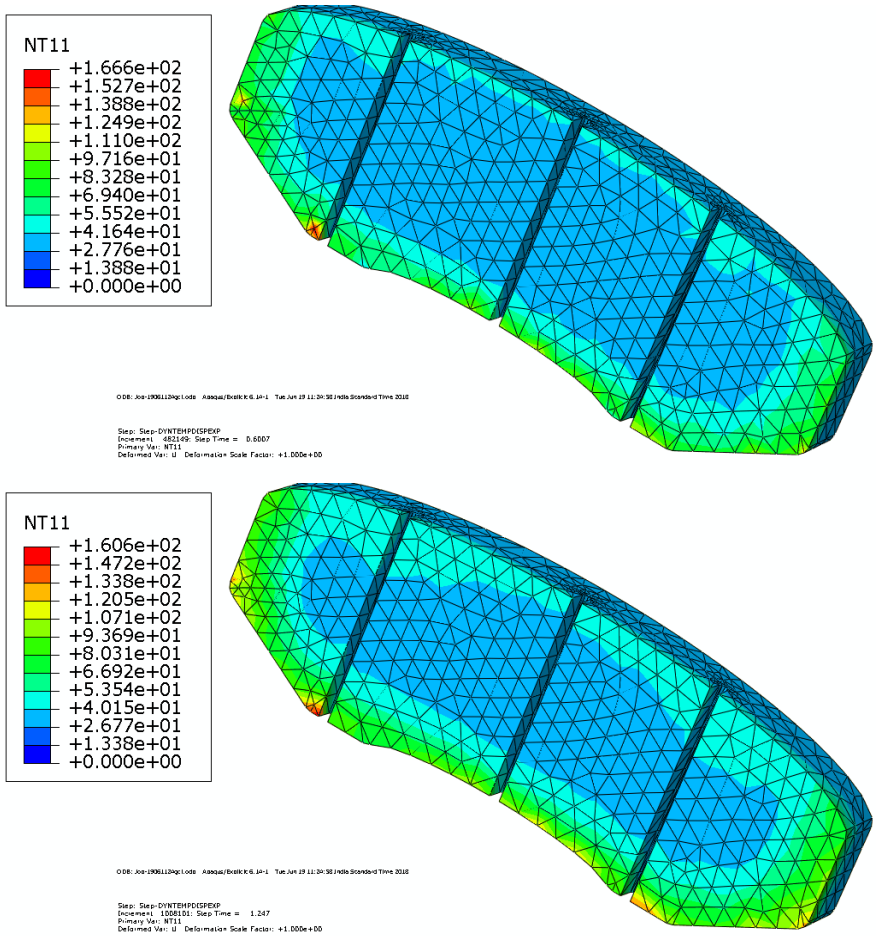

Fig. 4.18 Temperature distribution in friction pad

4.6 COMPARISON OF ANALYTICAL AND NUMERICAL RESULTS

The numerical analysis has been performed for 4 different materials i.e. ALMMC, DCI, GCI and MSS by the dynamic temperature displacement explicit analysis of disc brake using ABAQUS 6.14. The comparison between numerical and analytical results is obtained for the maximum temperature conditions for the different materials. The maximum temperature attained along with their corresponding time is given in table 4.5. The analytical results are found using Rudolf Limpert equation for single stop braking for a solid rotor. Some variations are found in the temperature obtained using analytical and numerical simulation methods. This may be due to the assumptions made, but the variations are within the limits thus proving the validation of the simulation.

From the table 4.3 this can be concluded that MSS can't be used as the disc material in high mass vehicles with higher power capacity, since the temperature values may exceed the failure limit.

Table 4.3 Comparison of analytical and simulation temperature

Materials	Maximum temperature by simulation (^{o}C)	Time (s)	Analytical temperature values (^{o}C)	Error percentage (%)
ALMMC	101.3	0.75	94.1	7.1
DCI	99.1	0.82	96.2	2.9
GCI	112.2	0.91	103.2	8.1
MSS	128.1	0.76	122.34	4.5

CHAPTER 5

CONCLUSIONS

On the basis of above simulation results, the following conclusions can be drawn

1- In all the materials, i.e., ALMMC, DCI, GCI and MSS, maximum temperature occurs almost in the middle time of the braking phase. This is due to the fact that the braking power is maximum at the start of the braking and decreases with time.

2- In all the materials, i.e., ALMMC, DCI, GCI and MSS, temperature gradients are higher near the frictional contact region of brake surface and pads as compared to other regions. When the portion of disc comes in contact region, it gets heated in that duration. This results in high temperature gradients. But when the same portion rotates to complete the cycle, heat is distributed and more uniformity is seen in the temperature profile.

3- Always higher temperature occurs on the surface of the disc as compared to the inner material regions. This is due to that fact the time for the hard braking is less, and also heat is generated on the surface, so enough time is not available to bring uniformity of inner volume temperature.

4- The results of the maximum temperatures obtained by simulations are given below

ALMMC-101.3^{o}C

DCI-99.1^{o}C

GCI-112.2^{o}C

MSS-128.1^{o}C

This can be concluded that the maximum temperature is observed in the Martensitic stainless steel case with a value of 128.1^{o}C. This is due to the minimum thermal diffusivity of the MSS resulting in more storage and highest temperature.

5- The kinetic energy of the disc is decreasing almost linearly in the initial braking phase and then the rate of decrease decreases till stop. This can be attributed to the variation of

coefficient of friction with temperature. Coefficient of variation increases till 150-200^{o}C temperature and then decreases further.

6- Maximum temperature for all the materials always occurs in the frictional contact region of the disc and the pads.

7- Temperatures are higher in the ring contained by disc and friction pads, and decreases both above and below it. Since more contact of the pad is in outer radius region of the disc, so higher temperatures are observed in outer radius region as compared to inner radius region.

8- Saw-tooth variation of temperatures is observed in the nodes present in frictional contact ring which denote the sudden increase of temperature as soon as the node enters in the contact region and decrease further with time due to thermal diffusion during completion of the rotation cycle. This variation is almost similar to the variation observed experimentally.

9- Role of convection and radiation heat transfer is negligible, since the braking time is less under hard braking conditions.

10- In the friction pads, higher temperatures could be seen on the outer periphery of the surface. This is due to the fact that there is a cross-section change and hence area is less which results in higher temperatures.

11- In the bottom region of outer periphery of the friction pads, higher temperatures are observed as compared to the top region because of the higher contact area in bottom of the pads.

12- Highest rate of rise of temperature is observed in the MSS material followed by GCI, DCI and ALMMC. The main cause of this is the lowest thermal diffusivity of the MSS.

13- Rise of temperature is uniform for ALMMC which can be seen through the saw tooth temperature diagram as compared to other materials. In case of MSS, the rise is higher and non-uniform. This can be attributed to lower thermal diffusivity and thermal conductivity.

14- As can be seen in the saw-tooth figures, the decrease of temperature near the completion of the rotation cycle is greatest for ALMMC. For other materials, the decrease is lower owing to their lower thermal diffusivity.

15- In MSS, the temperature is more concentrated in few regions. The variation of temperature within the disc thickness is highest. The higher temperature is in few regions while the rest of the material is at comparatively lower temperatures.

16- In ALMMC material, the variation of temperature within the disc thickness is less. Heat is more distributed in all the regions. Higher portion of the materials can be seen with the same colour.

17- The DCI and GCI material are showing almost the same type of temperature results and distribution. But GCI is used in disc brakes of the cars due to the manufacturing ease and hence a reduction in the total cost.

18- MSS is the best material in case of light power bikes since the braking power is low and the material will sustain those temperatures. For high end cars, etc. MSS may not be suitable because of the lower thermal diffusivity resulting in very high temperatures.

19- ALMMC provides an alternative to the conventional disc materials because of its high thermal diffusivity, but strength is a criterion which needs to be worked upon.

FUTURE SCOPE

In this work a solid model of the disc is analyzed numerically for different materials along with the analytical result. The future continuation of the work could include developing and analyzing disc brakes having complex geometries and designs with numerical analysis along with experimental work on disc brake bench test equipment. There is a scope of including CFD analysis to include actual convection heat transfer based on the design and geometry. Development of material can be considered to provide better properties which can result in higher life, wear resistance, thermal conductivity, thermal fatigue resistance, etc. More work can be done on composite materials of Aluminium alloy as they provide higher fuel efficiency by reducing the weight of the vehicle.

REFERENCES

[1] Dr. Kirpal Singh, Automobile Engineering Volume 1, Standard Publishers Distributors, Delhi, pp. 309-394, 2011.

[2] https://www.dummies.com/home-garden/car-repair/brakes-bearings/how-to-check-disc-brake (Retrieved 20/06/2018).

[3] HB Yan, QC Zhang, TJ Lu, "Heat transfer enhancement by X-type lattice in ventilated brake disc," International Journal of Thermal Sciences, pp. 39-55, January 2016.

[4] Rudolf Limpert, Brake Design and Safety, Third edition, SAE International, pp. 1-112, 2011.

[5] https://www.quora.com/What-is-the-difference-between-fixed-and-floating-caliper (Retrieved 20/06/2018).

[6] Rajesh Kumar, "Transient Thermoelastic analysis of Disk Brake using Ansys Software," M.tech thesis, Thapar university, 2008.

[7] http://www.aa1car.com/library/disc_brakes.htm(Retrieved 20/06/2018).

[8] http://www.pro-touring.com/threads/101215-fixed-vrs-floating-Calipers (Retrieved 20/06/2018).

[9]http://www.thecartech.com/subjects/auto eng2/Auto_Eng1.htm(Retrieved20/06/2018)

[10] R. Udayakumar and Ramesh Ponnusamy, "Computer Aided Design and Analysis of Disc Brake Rotors for Passenger Cars," 2013 International Conference on Computer Applications Technology, January 2013.

[11] ASM International Handbook Committee, Casting ASM handbook, Volume 15, ASM International, 2008.

[12] https://www.quora.com/Why-is-gray-cast-iron-a-brittle-material.

[13] Harold T Angus, Cast iron: physical and engineering properties, 2nd edition, Butterworths publishers, 2007.

[14] Ductile iron marketing group, Ductile Iron Data for Design Engineers, published by RIO TINTO IRON AND TITANIUM INC., 1990.

[15] William D Callister, Jr, (1997). Materials science and engineering: An introduction, 7th edition, published in New York: John Wiley & Sons, 2007.

[16] Pulkit Bajaj, "Mechanical Behaviour of Aluminium based metal matrix composites reinforced with SiC and Alumina," M.Tech thesis, Thapar university.

[17] Ankit Tyagi and Deepak Sharma, "Characterization of AA6082/Si3N4 Composites," 1st International Conference on New Frontiers in Engineering, Science & Technology, New Delhi, January 2018.

[18] Nagesh S.N, Siddaraju C, S V Prakash and M R Ramesh, "Characterization of Brake pads by variation in composition of friction material," International Conference on Advances in Manufacturing and Materials Engineering, pp. 295-302, December 2014.

[19] M.A. Maleque, S. Dyuti and M.M. Rahman (*Member, IAENG*), "Material Selection Method in Design of Automotive Brake Disc," Proceedings of the World Congress on Engineering 2010, Volume 3 WCE 2010, June 30 - July 2, 2010.

[20] Agustin Salazar, "On thermal diffusivity," European Journal of Physics, pp. 351-358, 2003.

[21] A. Belhocine, M. Bouchetara, "Temperature and Thermal Stresses of Vehicles Gray Cast Brake," Journal of Applied Research and Technology, Volume 11, Issue 5, pp. 674-682, October 2013.

[22] Sung Pil Jung, Young Guk Kim and Tae Won Park, "A Study on Thermal Characteristic Analysis and Shape Optimization of a Ventilated Disc," International Journal of Precision Engineering and Manufacturing, Volume 13, Issue 1, pp. 57-63, January 2012.

[23] Pyung Hwang1 and Xuan Wu, “Investigation of temperature and thermal stress in ventilated disc brake based on 3D thermo-mechanical coupling model,” Journal of Mechanical Science and Technology, Volume 24, Issue 1, pp 81–84, January 2010.

[24] Daanvir Karan Dhir, “Thermo-mechanical performance of automotive disc brakes, Materials Today: Proceedings,” Volume 5, Issue 1, Part 1, pp. 1864-1871, 2018.

[25] Qifei Jian and Yan Shui, “Numerical and experimental analysis of transient temperature field of ventilated disc brake under the condition of hard braking,” International Journal of Thermal Science, Volume 122, pp. 115-123, December 2017.

[26] A. Yevtushenko and E. Ivanyk, “Determination of heat and thermal distortion in braking systems,” Wear, Volume 185, Issues 1-2, pp. 159-165, June 1995.

[27] A.A. Yevtushenko, A Adamowicz and P. Grzes, “Three-dimensional FE model for the calculation of temperature of a disc brake at temperature-dependent coefficients of friction,” International Communications in Heat and Mass Transfer, pp. 18-24, March 2013.

[28] Andrew Day, Braking of Road Vehicles, Published by Elsevier Inc, pp. 215-235, 2014.